FINAL REPORT

DEVELOPMENT OF AN IMPROVED CAPABILITY FOR PREDICTING THE RESPONSE OF HIGHWAY BRIDGES

by

F. W. Barton
Faculty Research Scientist

and

W. T. McKeel, Jr.
Research Scientist

(The opinion, findings, and conclusions expressed in this report are those of the authors and not necessarily those of the sponsoring agencies.)

Virginia Highway & Transportation Research Council
(A Cooperative Organization Sponsored Jointly by the Virginia Department of Highways & Transportation and the University of Virginia)

In Cooperation with the U. S. Department of Transportation
Federal Highway Administration

Charlottesville, Virginia

June 1986
VHTRC 86-R45

BRIDGE RESEARCH ADVISORY COMMITTEE

L. L. MISENHEIMER, Chairman, District Bridge Engineer, VDH&T

J. E. ANDREWS, Bridge Design Engineer Supervisor, VDH&T

G. W. BOYKIN, District Materials Engineer, VDH&T

C. L. CHAMBERS, Division Bridge Engineer, FHWA

C. D. GARVER, JR., Division Administrator -- Construction Div., VDH&T

M. H. HILTON, Senior Research Scientist, VH&TRC

J. G. G. MCGEE, Assistant Construction Engineer, VDH&T

M. F. MENEFEE, JR., Structural Steel Engineer, VDH&T

R. H. MORECOCK, District Bridge Engineer, VDH&T

C. A. NASH, JR., District Engineer, VDH&T

F. L. PREWOZNIK, District Bridge Engineer, VDH&T

W. L. SELLARS, District Bridge Engineer, VDH&T

F. G. SUTHERLAND, Bridge Engineer, VDH&T

L. R. L. WANG, Prof. of Civil Engineering, Old Dominion University

ABSTRACT

This study compared experimental and analytical stress and deflection response of a simply-supported highway bridge as measured from a field test and as predicted from a finite-element analysis. The field test was conducted on one span of a six-span highway bridge in Virginia using a loaded dump truck as the applied loading. Deflection and strain measurements were recorded at the quarter point and midspan of two adjacent spans with the test vehicle in various positions. A finite-element model of the bridge was then developed in which the bridge deck was represented using quadrilateral shell elements and the girders were represented by beam elements. Two different versions of the finite element model were utilized, one assuming simply-supported ends, and one in which continuity was included. Nodes were located such that stresses and deflections in the finite-element model could be predicted at locations corresponding to those where experimental data was recorded.

It was found that the measured response and predicted response from the finite element model with simply-supported boundaries did not compare favorably. Differences on the order of 50% or more were typical. Experimental data from the field test had, however, indicated a degree of restraint at the supports corresponding to approximately 10% fixity. When this degree of restraint was included in the finite element model of the bridge, comparison between measured and predicted response improved markedly. In fact, the difference between measured and predicted deflections were generally less than 5%. Comparison of measured and predicted stresses indicated somewhat larger differences although the agreement was still satisfactory.

Results of this study indicate that the overall response of a relatively simple bridge structure can be satisfactorily predicted from rationally developed finite element models. In the formulation of these models, however, considerable attention should be devoted to a realistic representation of the longitudinal and transverse stiffness and particularly to the support conditions of the structure.

FINAL REPORT

DEVELOPMENT OF AN IMPROVED CAPABILITY FOR PREDICTING THE RESPONSE OF HIGHWAY BRIDGES

by

F. W. Barton
Faculty Research Scientist

and

W. T. McKeel, Jr.
Research Scientist

INTRODUCTION

There are many areas of structural design in which completely rational procedures either are not feasible or require so many simplifying assumptions that the final formulations render results that are somewhat questionable. In such cases design engineers rely on judgement, intuition, and experience, in addition to calculations. In many instances where the problem is common enough, standard rules of design are developed, adjusted, and modified as the finished structure is observed and studied throughout its service life.

The traditional design of highway bridges is one such area in which engineering judgement and experience is essential. With safety and serviceability the primary considerations, every effort is made during the design process to include a number of implicit safety factors intended to account for uncertainties in materials, loads, fabrication details, and possible errors in construction. The utilization of conservative design procedures and the inclusion in the design of a significant factor of safety serve to protect the overall integrity of bridge against collapse and to ensure that it can operate safely at the designed service load with a high degree of confidence.

While these traditional design procedures result in bridge structures which are appropriately safe, when used for analysis purposes these same procedures predict capacities and strengths which are far less than the actual values for the structures. Thus, while appropriate for design, the traditional procedures of analysis and design are not satisfactory for determining the actual strength of a bridge system. There are a number of instances where a knowledge of the precise load capacity of a bridge is essential. For example, bridges are required to be posted when legal loads produce stresses in excess of the operating rating. The operating rating, however, is generally determined using the same analysis procedures that are used in the design process, and the predicted operating rating thus may be unrealistically low. This

practice results in bridges being posted unnecessarily or in posted limits being unnecessarily restrictive. An accurate assessment of the capacity of a bridge is also essential when the issuance of an overload permit for the structure is under consideration.

A knowledge of the true load capacity and strength of a bridge is also an essential element of any bridge repair and rehabilitation program. It is unrealistic to try to develop a priority list of structurally deficient bridges when there is uncertainty regarding the actual capacities of the structures. In addition, the rehabilitation scheme adopted usually will depend on the state of the structure; a severely deficient bridge might require one repair procedure while a moderately deficient might require some other repair approach.

Finally, there is the matter of the credibility of bridge and highway engineers as perceived by the highways users, the public, and elected officials. When a bridge is posted for a particular load level, it is not surprising to anyone when a vehicle whose weight far exceeds the posted limits safely passes over the bridge. Thus, declarations by highway officials regarding the limited capacity of a posted bridge or the unsafe state of another bridge tend to be disregarded by the public on the basis of experience.

While there would seem to be little justification for changing the procedures currently used in design, there does appear to be considerable justification for improving the procedures used in the analysis of bridge structures and, particularly, in those procedures used by bridge engineers in state Departments of Transportation and in consulting offices for predicting the capacity or rating of bridges.

In calculating stresses and deflections in large structural systems finite element models are generally used to represent the structure. Since analysis techniques are capable of analyzing such models exactly, errors in response are thus attributable to errors in modelling. Hence, the development of an improved capability for predicting bridge response translates directly into developing better finite element models of the bridge structures. This can most effectively be accomplished by using measured experimental responses of the actual structure as a basis for evaluating the results predicted by finite element models and for identifying those physical features of the bridge model that might realistically be modified to produce improved response predictions.

OBJECTIVES

The broad objective of this study was to develop an improved capability for the accurate and reliable prediction of stresses and deformations in bridges induced by prescribed loadings. The immediate goal was to provide the bridge engineer with an analysis tool that could

be used to determine the service load capacity on one type of bridge structure common on Virginia highways and of interest to the Virginia Department of Highways and Transportation. A longer-term goal was to enable bridge engineers to determine, with confidence, whether or not a prescribed overload could safely be permitted to pass over a particular bridge.

The basic thrust of this study was to develop an improved finite element model of the bridge selected for study. This model could then be used to compare the theoretical response of a bridge, as predicted by a computer analysis using this finite element model, with the actual, in-service response as determined from field tests. This comparison would then permit an evaluation of the effects of various parameters that might result in differences between predicted and measured responses, such as support conditions. Using results from the field test as a guide, appropriate modifications could subsequently be made to computer models until the predicted and measured responses would compare favorably. The final computer model should then provide the bridge engineer with an improved capability for assessing bridge responses under any loading condition.

The field test was conducted on only one highway bridge. The test structure was a six-span bridge with each span simply supported. Stresses and deflections at various locations in two of the spans were recorded for a variety of load cases.

Preliminary computer models of the bridge structure were developed based on a knowledge of the bridge geometry and the capability of the finite element codes available. Modifications were then made to the preliminary models to obtain results that were consistent with the field test data. The individual effect of each parameter on model response was observed. The final computer model then consisted of modifications to the preliminary model which produced results similar to those measured experimentally.

EXPERIMENTAL PROGRAM

Description of Test Structure

The test structure was a six-span bridge carrying state Route 276 over the North River one mile north of Weyers Cave, Virginia. The structure has a clear roadway width of 24 ft and a center-to-center bearing length of 66 ft 5 in in each simply-supported span. The bridge is comprised of a 7-1/2 in concrete slab on four W 36 x 160 steel girders with helical steel shear connectors used to provide composite action. The ends of the girders are simply supported using slotted bearing plates with anchor bolts attached to the flanges in such a manner as to allow free rotation. The substructure consists of a south abutment of gravity

type supported on steel piles, five piers, and a north shelf-type abutment founded on solid rock. Only the southern two spans of the structure were instrumented and tested. The structure is on a tangent and a very flat vertical curve. The road approaches are of bituminous macadam construction. A plan and elevation of the bridge is shown in Figure 1, a transverse section in Figure 2, and photographs of the test site and structure in Figures 3, 4, and 5, respectively.

The structure was designed in accordance with AASHO Standard Specifications, 1953 for H20-44 and H15-S12-44 loading. Construction was completed in August 1957 and the testing took place in June 1983.

This bridge was chosen as the test structure because the low traffic volume on Route 276 simplified instrumentation and, more importantly, minimized traffic congestion during the testing, when traffic flow had to be intermittently interrupted. Since the two test spans were over dry land, instrumenting the structure was relatively simple. Ladders and scaffolding allowed easy access to the underside of the structure without interference from traffic. Also, the instrumentation vehicle housing the electronic strain measuring equipment could be parked under one of the two test spans on the south end of the bridge.

Finally, in August and September of 1961 this same bridge had been subjected to a similar type of test by the Virginia Highway and Transportation Research Council.(1) It was anticipated that the previous test data, which were readily available, would be useful during the planning stage prior to the June 1983 field test and could also be used for subsequent comparison to perhaps identify changes in behavior. All of these factors made this bridge on Route 276 north of Weyers Cave particularly suitable as the test structure.

Instrumentation

The Federal Highway Administration provided the instrumentation, directed its installation, and operated the equipment for testing. The equipment included an instrument trailer outfitted with a strain measuring system and a deflection measuring system. The strain measuring system consisted of a 100-channel B & F, Model 161, Digital Data Logger capable of permanently recording the output of the strain gages. Forty-one strain gages (Micro-measurements, Model CEA-06-250UW-120) were placed on the girders and eleven concrete strain gages (Micro-measurements, Model EA-06-20CBW-120) were placed on concrete elements, six on the slab and five on the railing and sidewalk. Photographs of the Digital Logger and the two types of strain gages are shown in Figures 6, 7, and 8.

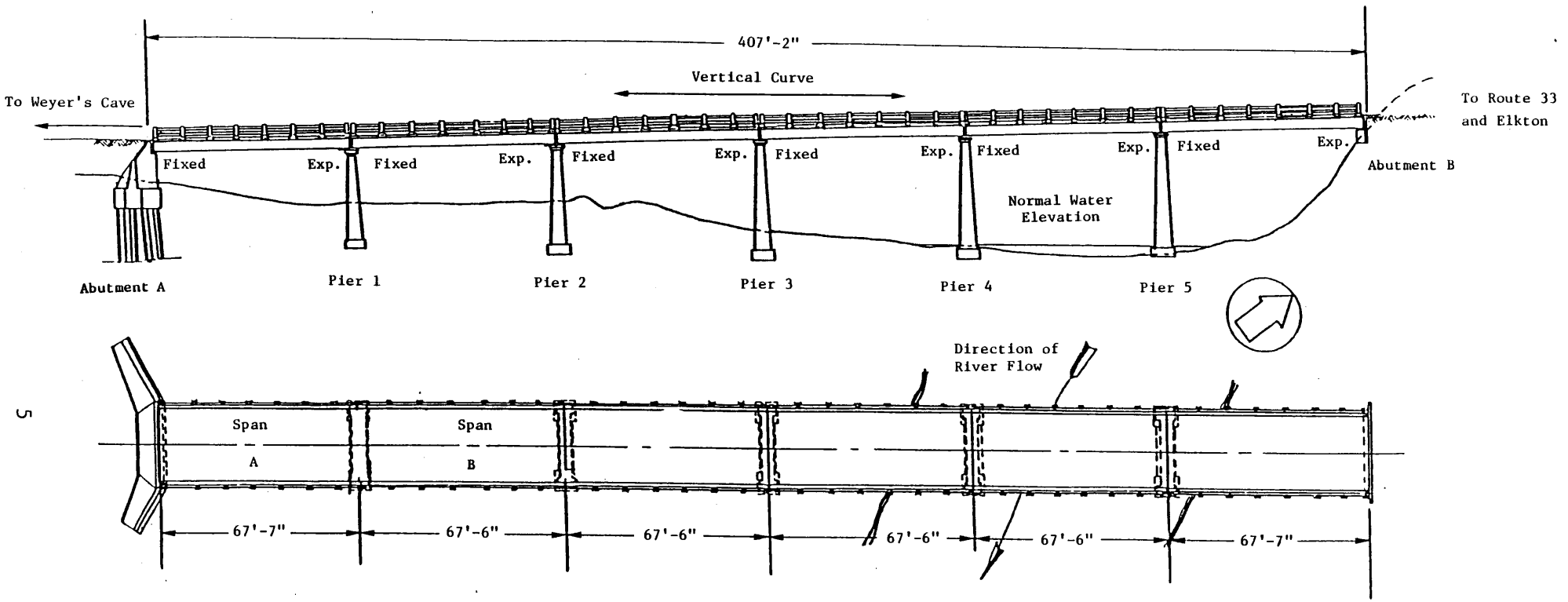

Figure 1. Profile and plan of Weyer's Cave Bridge, indicating test sections.

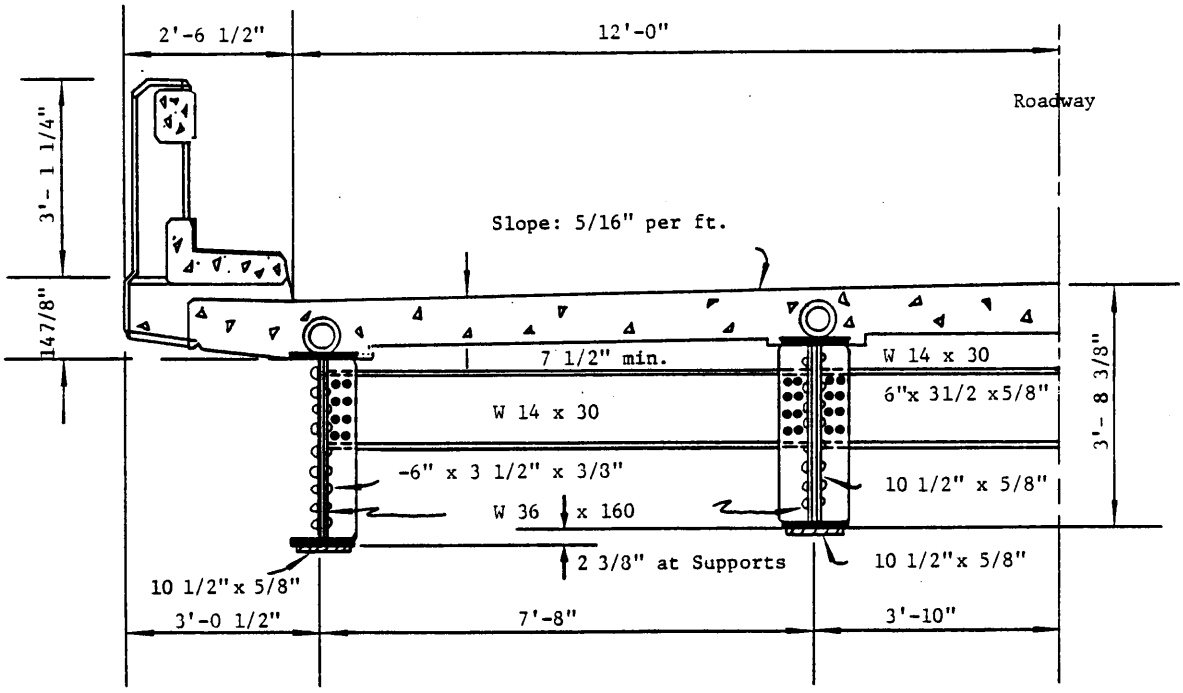

Figure 2. Half transverse section.

Figure 3. Photograph of test structure from the northbound approach.

Figure 4. Photograph of test site.

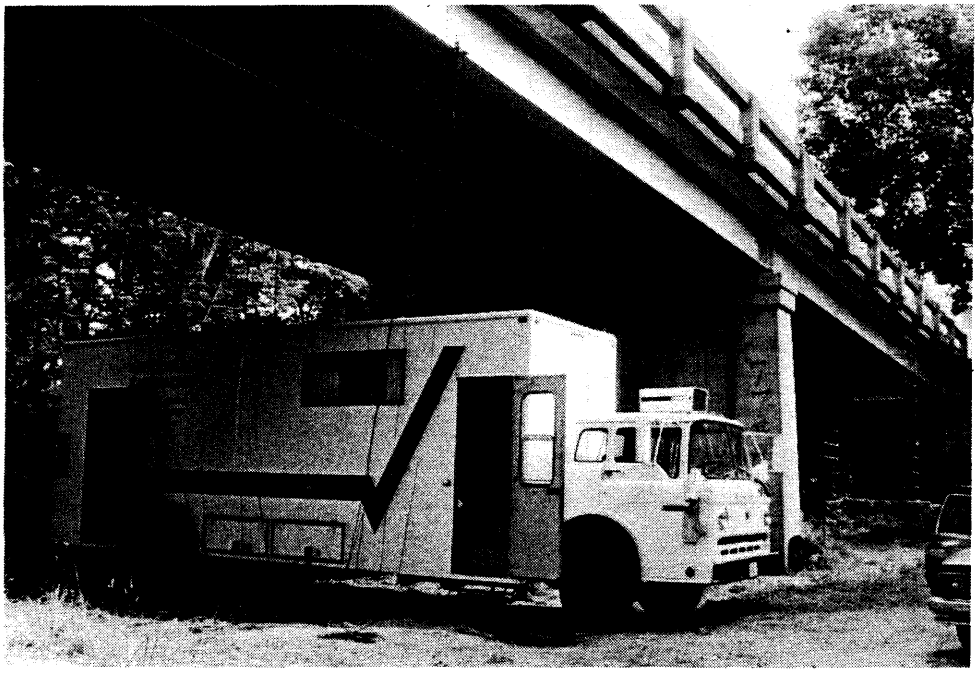

Figure 5. Photograph of instrumentation van and structure.

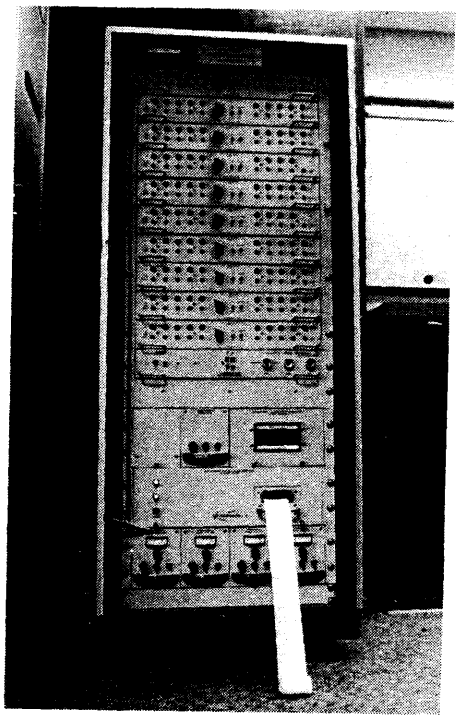

Figure 6. Photograph of digital data logger.

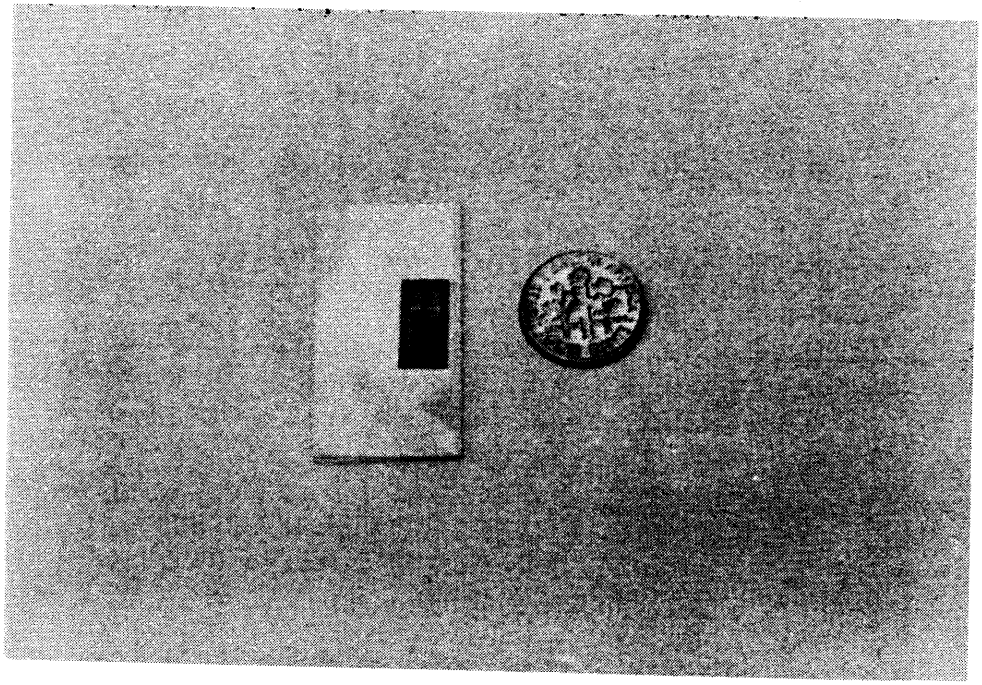

Figure 7. Photograph of steel strain gage.

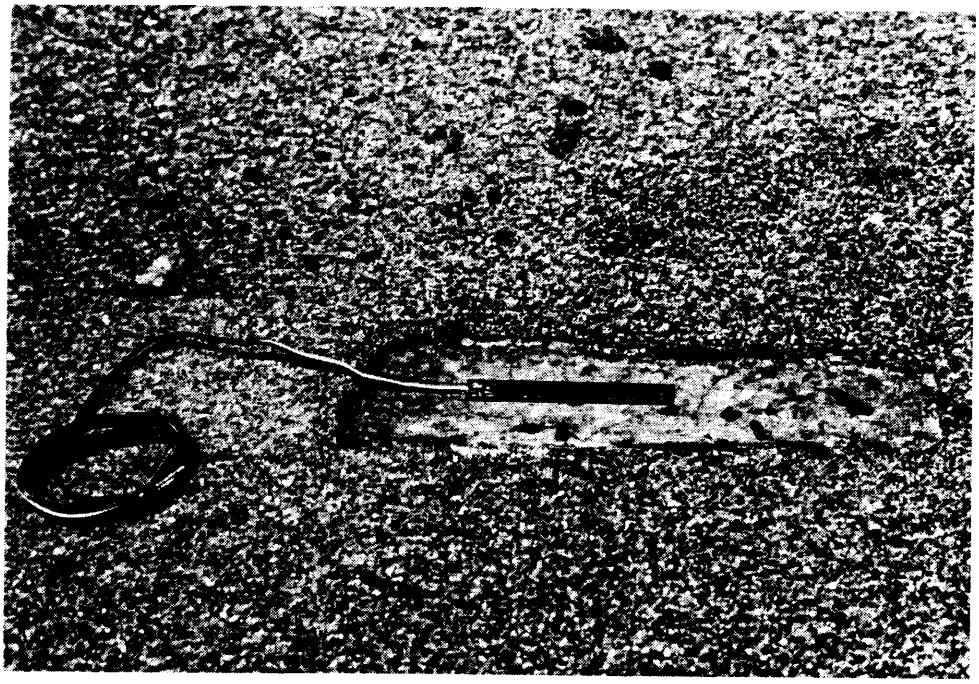

Figure 8. Photograph of concrete strain gage.

The forty-one gages used for strain measurements on the steel girders were placed at various flange and web positions at five transverse sections along the two test spans. These locations will be referred to as sections 1 through 5. For convenience, the span adjacent to the south abutment was designated as span A and the second span as span B. Section 1 was at the centerline of span A, while the remaining gage lines were in span B. Section 2 was located 13 ft 9 in from the centerline of the south bearings, 6 in off the termination of the cover plate. Section 3 was located 17 ft from the centerline of the south bearings on the full cover plate, 5 in inside of the beginning of the tapered nose. Section 4 was at the centerline of the span and Section 5 was 12 in from the centerline of the south bearing. The locations of these five gage lines are shown in Figure 9 and the placement of the strain gages along each section is shown in Figure 10. As indicated in Figure 10, strain gages were placed on the lower flanges of all girders at all five sections, on the top flanges of all girders at sections 2, 3 and 4, and on the webs of the girders 12 in from the lower flange at sections 4 and 5. Three gages were placed on the lower face of the slab at sections 2 and 4. A total of five concrete strain gages were placed on the curb and sidewalk at section 4, three on the west side and two on the east.

All gages measured strains in the longitudinal direction; it was assumed that the transverse strain was negligible. Stresses were computed from these strains by assuming a modulus of elasticity of steel (E_s) of 30,000,000 psi and a modular ratio (E_s/E_c) of 8, where E_c is the modulus of elasticity of concrete.

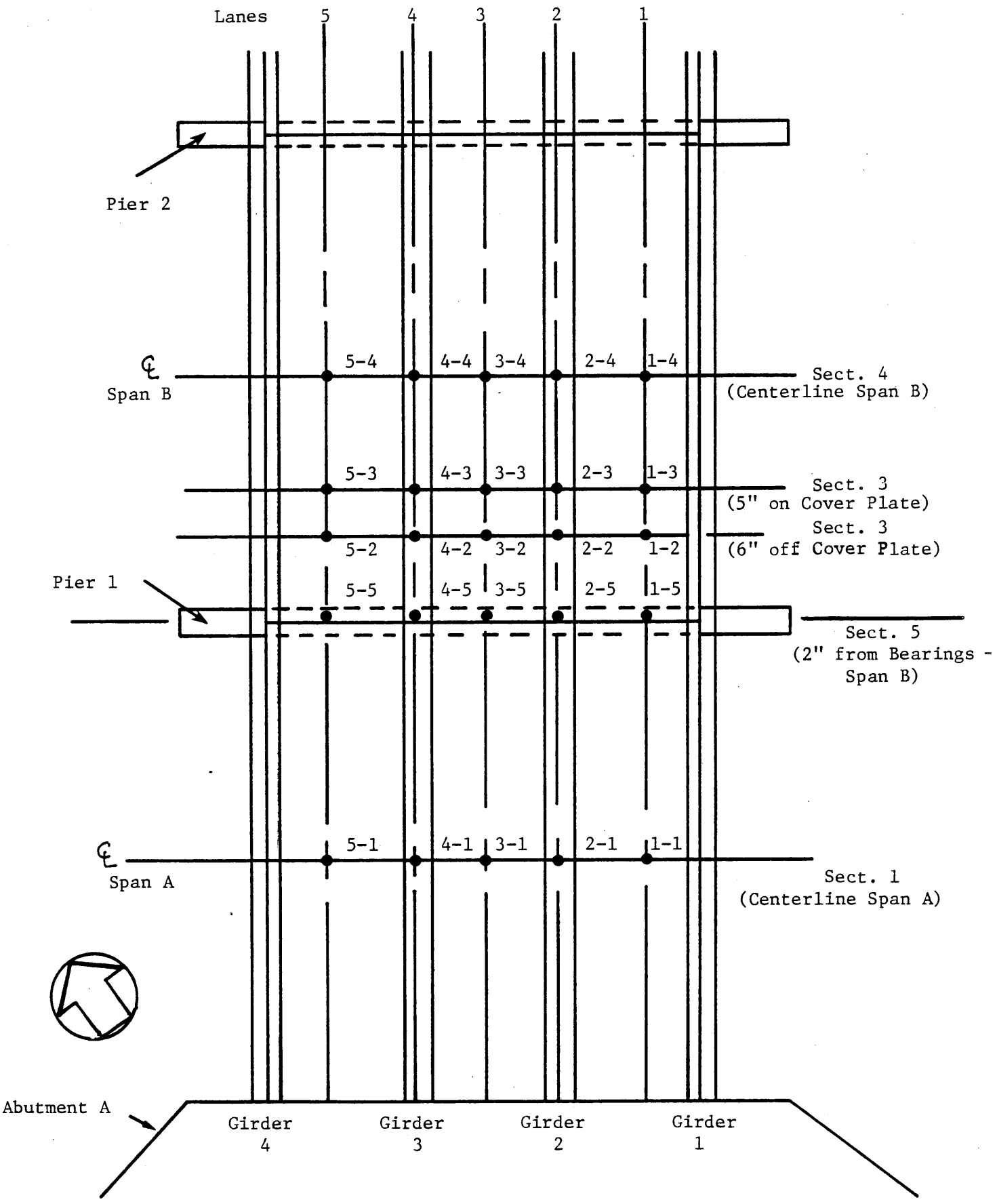

Figure 9. Sketch showing five strain gage sections along the two spans. Indicates load case.

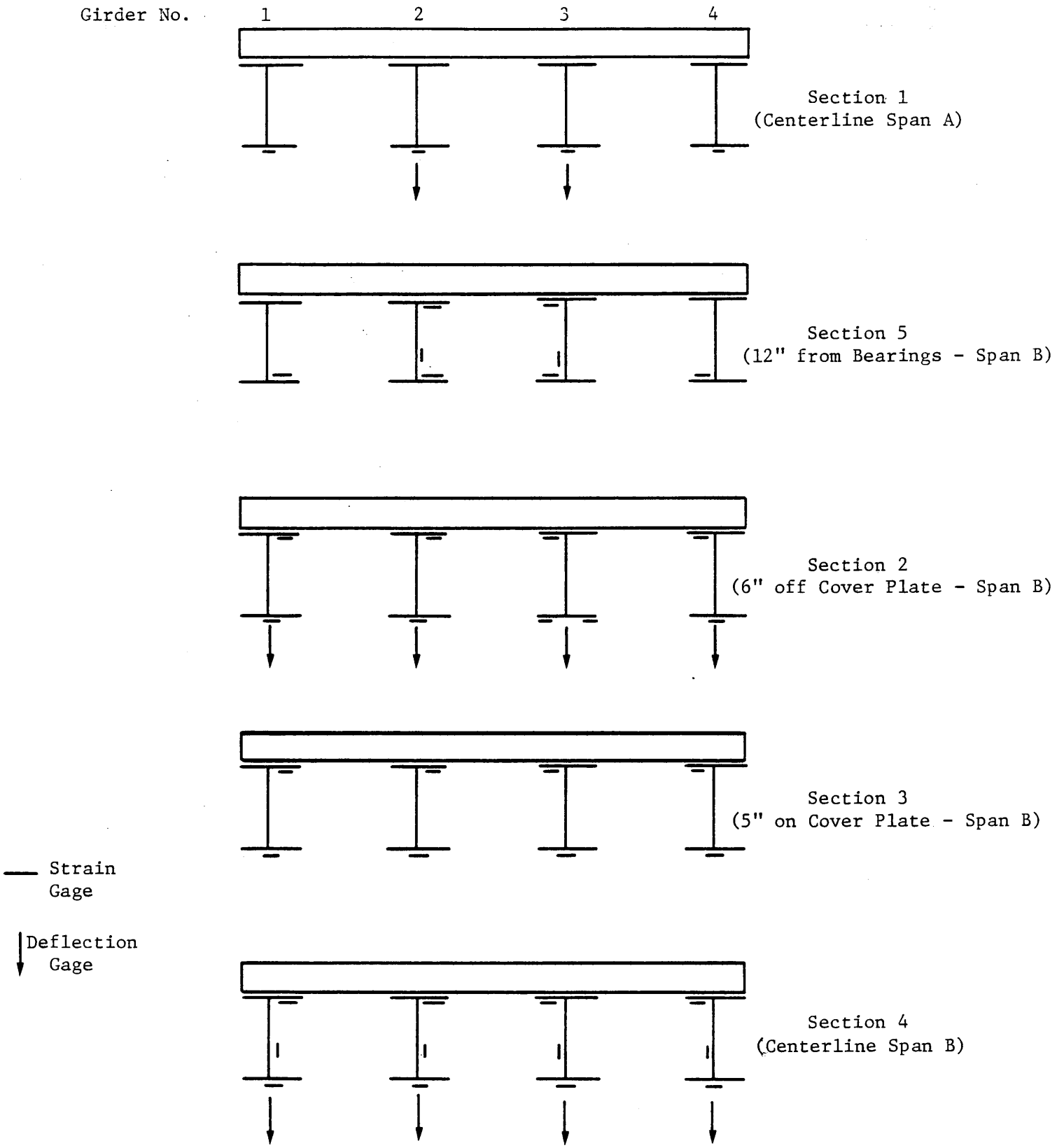

Figure 10. Sketch of gage locations for the five sections.

The deflection measuring system consisted of a Strainsert, Model WD1, static strain indicator and ten deflection gages fabricated in the Federal Highway Administration laboratories. The deflection gages consisted of a metal strip with one end clamped to the lower flange of the steel stringers and the other end anchored in a deflected position to the ground. A strain gage attached to the clamped end of the cantilever strip yielded strains proportional to the deflection when the flange deflected. The strain readings recorded on the Strainsert static strain indicator were reduced to deflections in inches by a calibration curve for each gage which had been previously determined in the laboratories of the Federal Highway Administration.

Sketches of the deflection gage positions are shown in Figure 10 and a photograph of a typical deflection gage is shown in Figure 11. Deflections were measured at midspan for all four girders in span B, at midspan for the two interior girders in span A, and at the quarter point (section 2) of all four girders in span B.

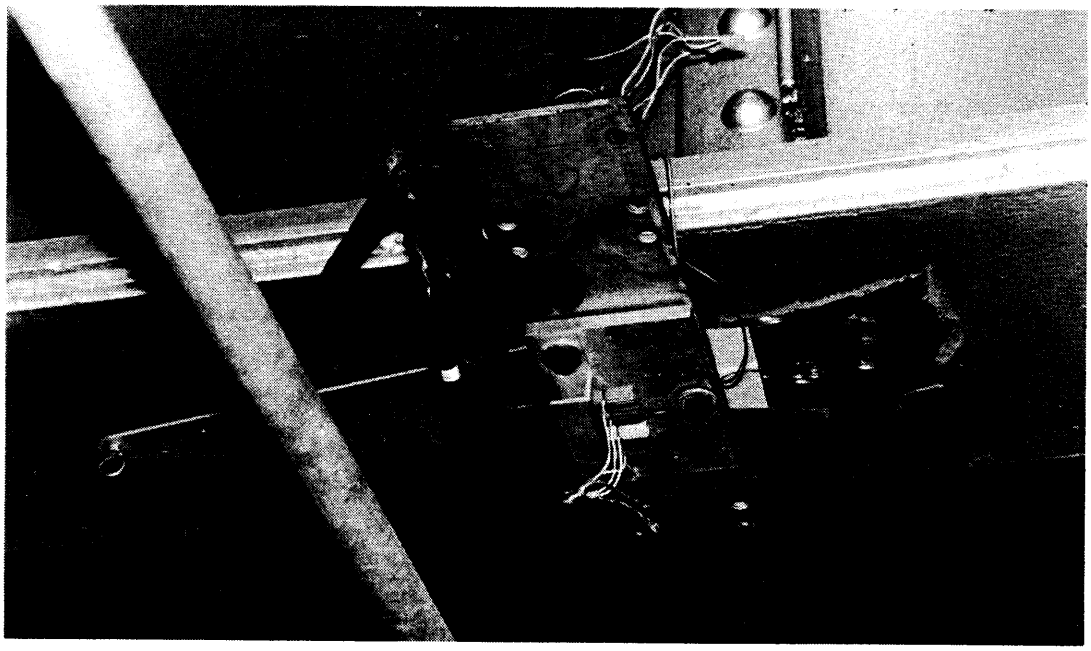

Figure 11. Photograph of a deflection gage.

Test Procedure

The test vehicle was a three-axle dump truck supplied by the Staunton District Office of the Virginia Department of Highways and Transportation and filled with gravel to obtain a gross weight of 57.22 kips for the bridge loading. A photograph of the truck and sketches giving dimensions between wheels and axles and wheel loadings are shown in Figures 12 and 13.

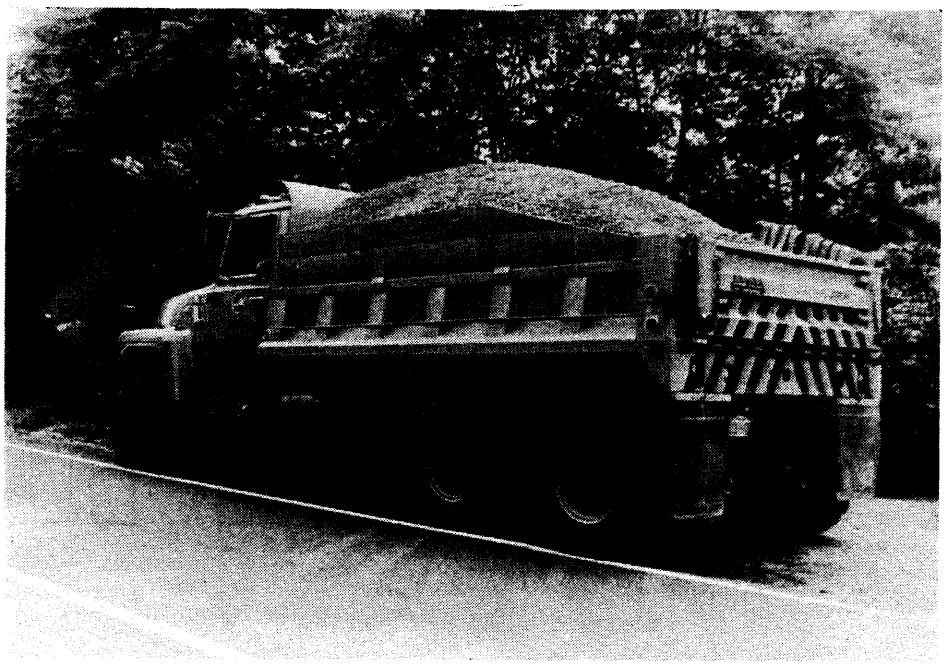

Figure 12. Photograph of the loading vehicle.

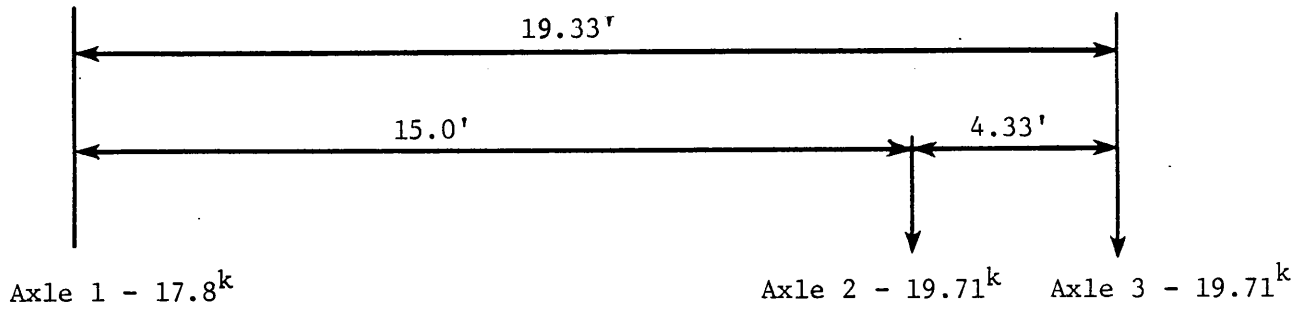

Axle Loads and Spacing

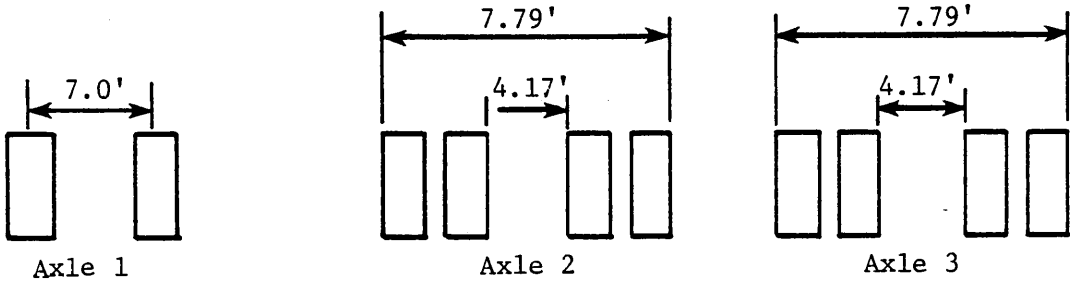

Transverse Wheel Spacing

Figure 13. Sketch showing dimensions and loads od test vehicle.

The test procedure involved successively placing the test vehicle at 25 locations in the two test spans and recording strains and deflections for each loading location. The 25 loading locations were defined by the intersection of five longitudinal lanes and the five transverse gage sections along each lane. At each load position, the test vehicle was placed such that the centerline of the truck at axle 2 was over the load point. For convenience in referencing, each load position is identified by two numbers in which the first number denotes the lane and the second number the transverse gage section along the lane. Thus, load position 2-4 denotes the load vehicle in lane 2 at section 4. The five traffic lanes and the four girders are numbered sequentially from east to west. The lane positions were selected as follows:

1. Lanes 1 (east-curb) and 5 (west-curb) were located such that the rear wheels of the test vehicle were against the curb.

2. Lanes 2 and 4 were centered over girders 2 and 3, respectively

3. Lane 3 (centerline) was the centerline of the bridge roadway.

A sketch of the vehicle positioned in lanes 1, 2, and 3 is shown in Figure 14.

Recording of the strain and deflection data at each of the 25 loading positions was repeated four times, and the four sets of data were then averaged to account for drift and to obtain the final response data.

Test Results

As noted earlier, the primary purpose of the experimental program was to provide measured data as a basis for evaluating and developing improved computer models of the bridge. A secondary study objective was to determine how much, if any, the properties of the bridge had changed since the 1961 field test. It is of interest, however, to also use data to obtain an indication of the overall response of the structure in terms of deflection patterns and the transverse load distribution.

Fifty-two strain and ten deflection readings were tabulated for each of the 25 load positions. Experimental stress and deflection data for the lower flange gages of the four girders at three gage sections and three lane positions along span B are shown in Table 1. The data are tabulated for centerline (lane 3), east curb (lane 1), and west curb (lane 5) loadings at the three load positions. The data seem to be consistent with what would be expected and no obvious discrepancies were observed. Similar data for the stresses on the webs and top flanges are shown in Tables 2 and 3. The top flange stresses were low and sometimes slightly negative indicating that the neutral axis of the composite section was close to the top flange.

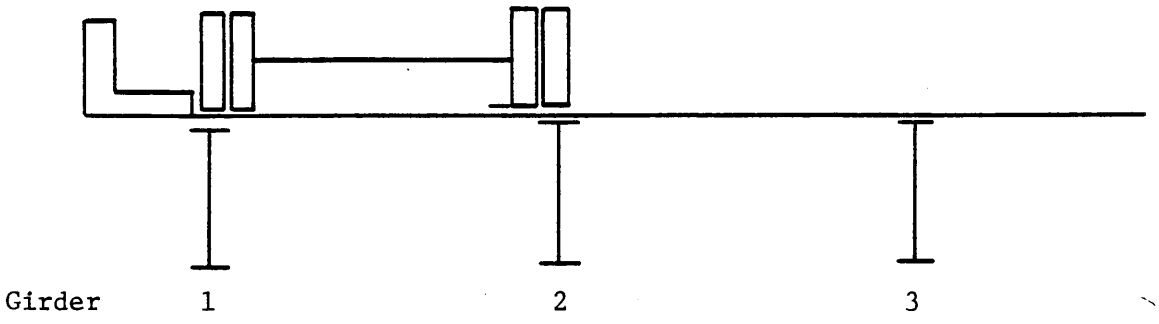

Lane 1. Rear Tandem Wheels Against Curb

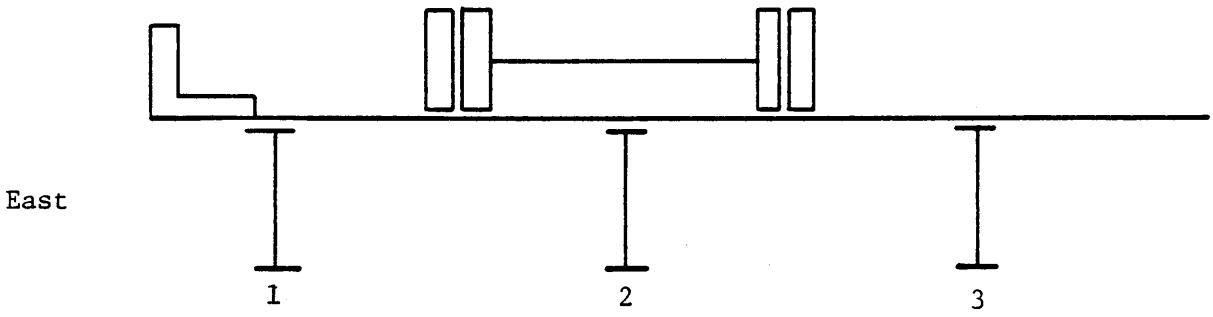

Lane 2. Centerline of Rear Randem Axles Coincides with Centerline of Girder.

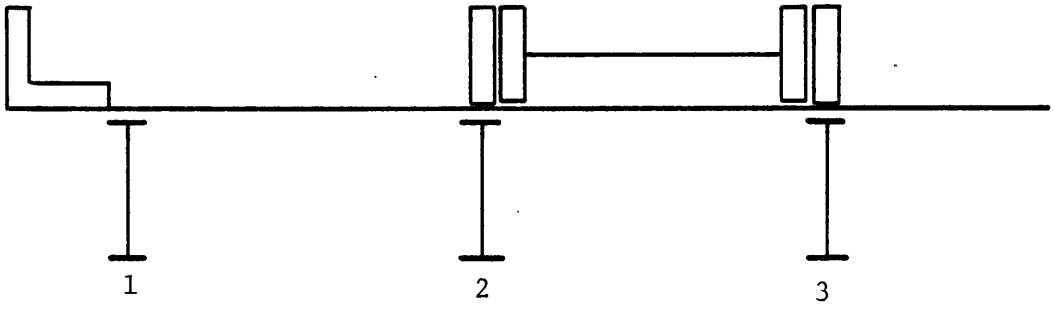

Lane 3. Centerline of Rear Tandem Axles Coincides with Centerline of Roadway.

NOTES: Lanes 4 and 5 Correspond to Lanes 2 and 1, respectively.

Figure 14. A detailed sketch of loading lane positions.

TABLE 1

Deflections and Maximum Stresses at Midspan

Girder	Load Case 3-2 Stress (psi)	Load Case 3-2 Deflection (in)	Load Case 3-3 Stress (psi)	Load Case 3-3 Deflection (in)	Load Case 3-4 Stress (psi)	Load Case 3-4 Deflection (in)
1	735	0.049	830	0.053	1,010	0.063
2	1,440	0.091	1,794	0.098	2,595	0.131
3	1,360	0.096	1,695	0.104	2,505	0.133
4	690	0.047	780	0.049	969	0.059
	Load Case 1-2		Load Case 1-3		Load Case 1-4	
1	1,790	0.102	2,180	0.117	2,980	0.147
2	1,419	0.085	1,810	0.102	2,680	0.132
3	714	0.050	819	0.058	1,050	0.072
4	150	0.011	204	0.011	204	0.012
	Load Case 5-2		Load Case 5-3		Load Case 5-4	
1	105	0.014	114	*	165	0.014
2	690	0.036	804	0.049	1,005	0.065
3	1,380	0.083	1,755	0.095	2,529	0.126
4	1,710	0.103	2,109	0.115	2,919	0.150

At Quarter Point - Five Inches on Coverplate (Section 3)

	Load Case 3-2		Load Case 3-3		Load Case 3-4	
1	495	---	510	---	504	---
2	1,530	---	1,794	---	990	---
3	1,539	---	1,809	---	990	---
4	585	---	600	---	609	---
	Load Case 1-2		Load Case 1-3		Load Case 1-4	
1	1,614	---	1,914	---	1,300	---
2	1,494	---	1,800	---	579	---
3	585	---	639	---	585	---
4	84	---	90	---	135	---
	Load Case 5-2		Load Case 5-3		Load Case 1-5	
1	69	---	75	---	84	---
2	600	---	540	---	594	---
3	1,470	---	1,770	---	1,005	---
4	1,950	---	2,310	---	1,494	---

NOTE: No deflection gages were placed at Section 3

(TABLE 1 continued)

At Quarter Point - Six Inches Off Coverplate (Section 2)

	Load Case 3-2		Load Case 3-3		Load Case 3-4	
1	609	*	669	0.028	600	0.029
2	2,370	0.068	2,454	0.073	975	0.069
3	2,372	0.064	2,442	0.070	1,014	0.062
4	549	0.031	570	0.042	504	0.032
	Load Case 1-2		**Load Case 1-3**		**Load Case 1-4**	
1	2,409	0.064	2,559	0.072	1,275	0.074
2	2,355	0.063	2,475	0.070	1,005	0.065
3	714	0.024	753	0.029	665	0.033
4	9	0.007	60	0.012	60	0.011
	Load Case 5-2		**Load Case 5-3**		**Load Case 5-4**	
1	159	0.007	159	*	180	**
2	675	0.031	744	0.021	660	0.022
3	2,250	0.051	2,367	0.061	1,040	0.060
4	2,475	0.069	2,634	0.072	1,314	0.071

* Data unavailable.

TABLE 2

Stresses at Midspan

Girder	Load Case 3-2 Stress (psi)	Load Case 3-3 Stress (psi)	Load Case 3-4 Stress (psi)
1	684	750	909
2	1,014	1,269	1,830
3	864	1,110	1,614
4	570	684	849
	Load Case 1-2	**Load Case 1-3**	**Load Case 1-4**
1	1,275	1,560	2,154
2	819	1,044	1,530
3	480	579	690
4	135	165	165
	Load Case 5-2	**Load Case 5-3**	**Load Case 5-4**
1	54	60	69
2	420	480	579
3	669	900	1,290
4	1,185	1,500	2,124

TABLE 3

Top Flange Stresses at Midspan

Girder	Load Case 3-2 Stress (psi)	Load Case 3-3 Stress (psi)	Load Case 3-4 Stress (psi)
1	---	---	---
2	159	150	84
3	54	60	120
4	-75	-99	-159
	Load Case 1-2	**Load Case 1-3**	**Load Case 1-4**
1	---	---	---
2	-99	-105	-135
3	-105	-150	-189
4	-45	-45	-114
	Load Case 5-2	**Load Case 5-3**	**Load Case 5-4**
1	---	---	---
2	225	249	384
3	-135	-69	-159
4	-45	-99	-174

NOTE: Girder #1 data were erroneous and were disgarded.

Table 4 shows the percentage distribution of the live load to each girder for centerline, east curb, and west curb loadings. The percentage values were determined based on the percentage of the total resisting moment produced in each girder calculated from stress measurements. This transverse live load distribution is plotted in Figure 15.

In comparing the results of this study with those from the 1961 field test, it was assumed that the elastic modulus of the steel had remained the same. The modular ratio (n), and therefore the concrete modulus, was one variable of interest. The modular ratio can be determined indirectly by knowing the moment of inertia (I) and the location of the neutral axis (c) of the composite cross section. The section modulus I/c can then be determined theoretically by the equation

$$I/c = M_a/\sigma ,$$

where

M_a = applied moment (inches-kips), and

σ = experimental stress at bottom face of girder (psi).

TABLE 4

Distribution of Live Load Stresses - Bottom Flange - Midspan of Span B

Girder No.	Composite Moment of Inertia	Stress (psi)	C (in.)	Resisting Moment in-Kips	% of Total Resisting Moment	Applied * Moment in-kips	Resisting/ Applied
			Load Case 3-4				
1	30,263	1,010	30.6	99	14.2		
2	31,109	2,595	31.2	2,587	36.2		
3	31,109	2,505	31.2	2,498	35.5		
4	30,263	969	30.6	958	13.6		
				7,042		9,418	74.8%
			Load Case 1-4				
1	30,263	2,980	30.6	2,947	42.9		
2	31,109	2,680	31.2	2,672	38.9		
3	31,109	1.050	31.2	1,047	15.2		
4	30,263	204	30.6	202	2.9		
				6,868		9,418	72.9%
			Load Case 5-4				
1	30,263	165	30.6	163	2.5		
2	31,109	1,005	31.2	1,002	15.2		
3	31,109	2,529	31.2	2,522	38.4		
4	30,263	2,919	30.6	2,887	43.9		
				6,574		9,418	69.8%

* Applied moment has been calculated in Appendix B from the field loading and basic statics.

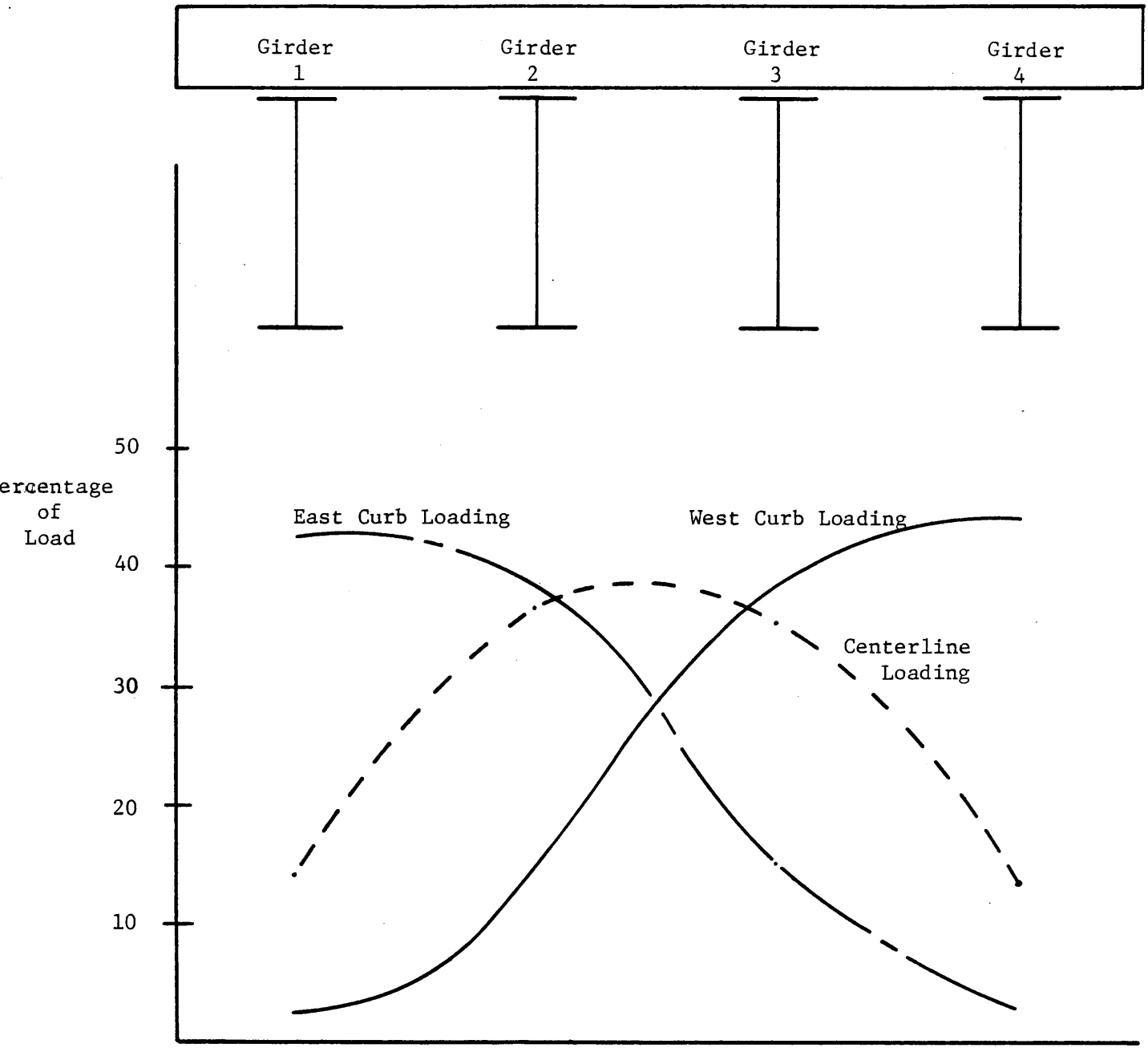

Figure 15. Graph showing the percentage of load distributed to each stringer at midspan of Span B for typical curb and centerline loadings.

Table 5 gives a comparison of the M_a/σ values, and therefore the I/c values, for the 1961 and 1983 studies. The applied moment was distributed to each of the four girders based upon the percentage of the total stress at each girder.

From the comparison of the values of M/σ for the 1961 and 1983 field tests, it is clear that the elastic properties of the bridge remained essentially constant. The small discrepancies between the 1961 and 1983 values are probably due to normal experimental error.

A detailed examination of the experimental data collected at the Weyers Cave bridge reveals some interesting characteristics. First, some slight antisymmetric responses to symmetric loads were observed. More importantly there appeared to be some degree of continuity at the bridge's "simple supports".

Table 6 shows responses to centerline loads. It would be expected that points symmetric to the centerline would show identical displacements and stresses. As the data show, mirrored positions along the centerline do not have identical displacements. This slight variation from symmetric behavior is rarely more than about 5%, and is probably the result of experimental error and slight nonuniformity in the bridge's construction. For this reason, no attempt was made to include this small deviation in the finite element models.

More significant is the identification of continuity at the bridge's simple supports. The evaluation of the field data showed that an approximation of the degree of continuity could be determined from the test results. Figure 16 and Table 7 summarize some basic supporting data for continuity at the hinged supports of the Weyers Cave bridge.

From the strain data in Table 7, it is observed that a load applied in span B produced a response in span A. Of particular interest was the amount of inter-span transfer along the girder lines. For example, load case 1-4 produced a strain of 99.33 at point A and -12.7 at point A'. The corresponding reading at point D was 6.8. This shows that more load was transferred along the same girder line to the next span than was transferred to the girder on the opposite side of the same span. This transfer occured along all girders for a load at any point on the span, and varied with the proximity of a girder line to the load point as indicated from the data in Table 7.

For load case 1-2, the strain in the lower flange at point B was 47.3 and at point B' it was -4.5. A transfer factor may be obtained by dividing the reading at B' by the reading at B. Such transfer factors can provide a rough estimate of the degree of continuity present at a particular simple support for a given load condition. In a similar fashion, transfer factors were developed for girder line 2 for the three remaining load conditions in Table 7. Table 8 shows the transfer factors calculated for each girder line for a given load test. Based on this approach, it may be noted that the transfer factor, or degree of fixity along the same girder line, was on the order of 10%.

TABLE 5

Comparison of (Applied Moment/Stress) Between 1963 and 1983

Girder No.	1963 Stress (psi)	1963 M(in-k)	1963 M f(in^3)	1983 Stress (psi)	1983 M(in-k)	1983 M f(in^3)
Load Case 3-4						
1	1,045 (16.44)	1,272	1,217	1,010 (14.27)	1,344	1,331
2	2,085 (32.81)	2,539	1,218	2,595 (36.66)	3,453	1,331
3	2,120 (33.36)	2,582	1,218	2,505 (35.39)	3,333	1.331
4	1,105 (17.39)	1,346	1,218	969 (13.69)	1,289	1,330
Sum	6,355	7,740		7,079	9,418	
Load Case 1-4						
1	2,780 (43.85)	3,394	1,221	2,980 (43.1)	4,059	1,362
2	2,235 (35.25)	2,728	1,221	2,680 (38.76)	3,650	1,362
3	1,100 (17.35)	1,343	1,221	1,050 (15.19)	1,431	1,363
4	225 (3.55)	275	1,222	204 (2.95)	278	1,363
Sum	6,340	7,740		6,914	9,418	
Load Case 5-4						
1	170 (2.57)	199	1,171	165 (2.49)	235	1,424
2	1,010 (15.17)	1,182	1,170	1,005 (15.19)	1,431	1,424
3	2,280 (34.47)	2,668	1,170	2,529 (38.21)	3,599	1,423
4	3,155 (47.69)	3,691	1,170	2,919 (44.11)	4,154	1,423
Sum	6,615	7,740		6,618	9,418	

NOTE: 1. The 1963 values are for the creep run for II15-S12 loading from Appendix B of the Weyer's Cave Bridge Dynamic Stress Study Report of 1963.

2. The values in parenthesis are the percentage of the total stress value.

TABLE 6

Centerline Loading Results

Girder							
1	2	3	4	1	2	3	4
Displacement (in)				Stress (ksi)			
.063	1.31	0.133	0.054	1.01	2.60	2.51	0.97
.029	0.69	0.062	0.032	0.60	0.98	1.01	0.50

Girders 1 and 4 symmetric
Girders 2 and 3 symmetric

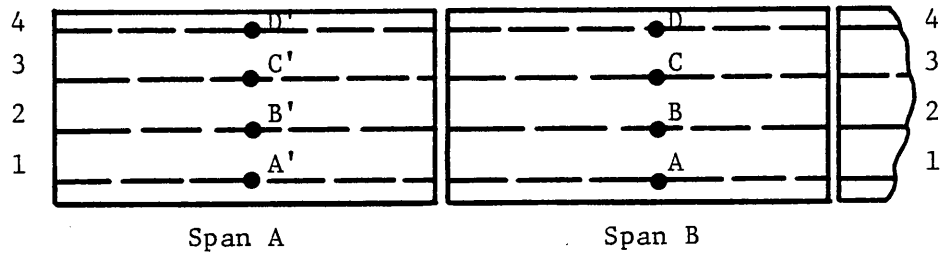

Figure 16. Girder location

TABLE 7

Continuity Data

Strain (in/in x 10^6)

Load Case	Span B				Span A			
	A	B	C	D	A'	B'	C'	D'
1-2	59.67	47.30	23.80	5.0	-9.0	-4.5	-4.5	-2.3
1-4	99.33	89.30	35.00	6.8	-12.7	-7.0	-6.8	-4.0
3-2	24.50	48.00	45.30	23.0	-8.0	-7.8	-6.0	-8.5
3-4	33.67	86.50	83.50	82.30	-9.8	-8.5	-8.0	-10.0

TABLE 8

Transfer Factors

Load Case	Girder Line			
	1	2	3	4
1-2	.15	.10	.19	.46
1-4	.13	.08	.19	.59
3-2	.32	.16	.13	.37
3-4	.29	.10	.10	.12

The continuity condition seems to have resulted from the imperfectness of the hinges used at the bridge supports. The type of supports used are shown in Figure 17. The effectiveness of this type of support as a hinge is dependent on the ability of the bearing plates to slip against each other. Proper lubrication is provided by a "permanent" lubricant impregnated into the bearing plates and protected by a bituminous material surrounding the bearing. When new, the bearing has a coefficient of friction of 0.1 or less, and is a fairly good approximation of a true hinge. With time, however, the bituminous protector breaks downs, exposing the mating surface of the bronze bearing plates to sand and salt. Further, the salt provides an electrolyte in which the bearing plate surfaces can rapidly corrode. This corrosion leads to a roughening or even fusion of the mating surfaces that considerably reduces the effect of the permanent lubrication. The Weyers Cave bridge is over 20 years old, and though its bearings appear to be structurally sound, the photograph in Figure 18 shows that they were not in ideal condition. This less than optimum condition was suspected to be the cause of the detected continuity. Such corroded bearings are particularly resistant to small rotations, which accounted for the larger percentage of girder transfer noted when a girder was away from the load point.

As will be seen in the next section of this report, inclusion of continuity at the supports in the analytical model of the bridge significantly improved the predicted response.

ANALYTICAL STUDY

The analytical portion of this study was undertaken primarily to evaluate the differences in responses predicted by typical finite element models of the structure and the responses determined from field tests. The evaluation was intended to provide some indication of how to develop improved models that would more accurately predict the overall response and capacity of a bridge structure than do the models presently used. This section of the report describes the development of the models used in this study, the response predicted by these models, a comparison of the predicted response and the measured response, and the effects of various model parameters that can be adjusted to improve model behavior.

The development of a "good" analytical model, for example a finite element model, which will be a rational representation of a bridge span and which will yield response data closely approximating the response of the actual structure, requires considerable judgement and experience. For example, the longitudinal stiffness of the bridge results from a contribution of both the girder and slab, particularly when the two act compositely as is usually the case. In defining the model, however, the actual bridge stiffness must be translated into an equivalent model stiffness by the use of such model parameters as elastic modulus, element depth or thickness, moment of inertia, torsional rigidity, interelement

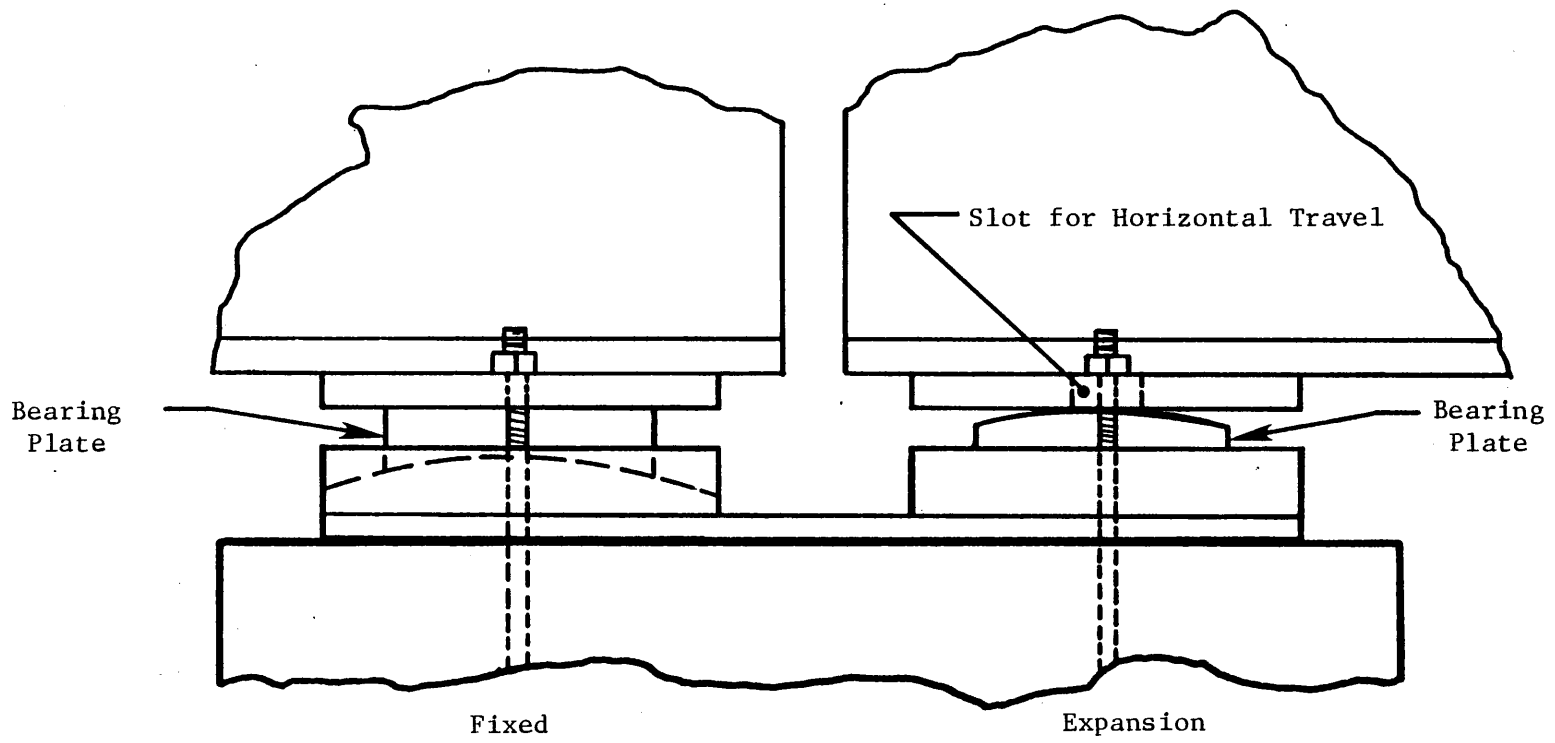

Figure 17. Bearing details.

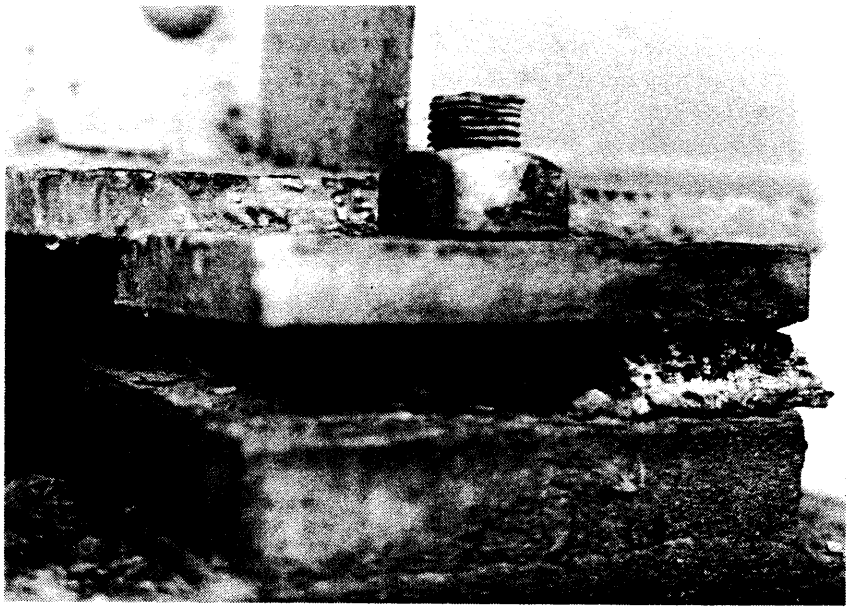

Figure 18. Condition of bearings.

connectivity, and similar features. It is also necessary to choose these model properties in such a way that the transverse behavior of the model, as well as the longitudinal behavior, simulates the actual response. The actual components that require incorporation into the model must also be identified. For example, clearly the primary load-carrying elements, such as the girders and slab, must be included. However, the necessity of modelling secondary components such as transverse stiffness and curb/railings is not clear.

The loading definition for the model is always an approximation. Finite element models generally require that loadings be specified in terms of nodal components, or sometimes surface pressures. Thus, in the case of a vehicle load on a deck surface, the wheel loads must be transformed into equivalent nodal loads in the form of concentrated forces and moments at the node points. If care is taken, however, the equivalent model loading should be representative of the actual loads imposed.

Finally, boundary conditions imposed on the model can only approximate the support conditions of the real bridge. Boundary conditions or constraints on finite element models typically entail prescribed values for generalized nodal displacements. For example, prescribing zero vertical displacement with no rotational restraint could represent an ideal pinned support or simply-supported end, while also specifying zero rotation could represent a fixed support. The types of bearings used in simply-supported bridge spans are never ideally simply supported but

always provide some degree of rotational and longitudinal restraint. In developing a good model, the problem is knowing what degree of constraint to use, and this generally entails an educated guess unless experimental evidence is available.

Model Development

All of the finite element models discussed in this section are representations of a single simply-supported span of the Weyers Cave bridge. Several models were developed and several variations of each were examined. All of the models will be briefly described, but detailed results will be provided only for those models that appeared to be the best in terms of predicting the actual response and in terms of being able to accommodate the inclusion of various bridge parameters. The two basic classes of models developed were a grillage model, made up of intersecting beams, and two variations of a traditional finite element model.

In the development and evaluation of the two finite models described, a number of model parameters were investigated to determine their overall effect on predicted responses. The factors considered included the mesh size, element and material properties such as the torsional stiffness, longitudinal and transverse composite action, modelling concepts for the girders, the role of transverse stiffness and curb/railing systems, the boundary conditions, and the number of necessary degrees of freedom at each node. Of these, only the inclusion of a composite curb/railing and continuity over the supports were found to have any significant effect on predicted responses and these are discussed subsequently.

As long as model parameters such as element geometry (e.g. stiffness), torsional restraint, and composite behavior were chosen and included in a rational manner, reasonable variations in these values had essentially no effect on response. With respect to nodal degrees of freedom, it was found that rotation about an axis normal to the deck (z-axis) and translation in the transverse direction (x-axis) could be restrainted with no measurable effect on response. Accordingly, these degrees of freedom were eliminated to reduce the problem size.

Finite element models frequently can be improved by refining the element mesh, and, ideally, as finer and finer mesh sizes are used, the results converge. Usually, the greatest improvement in model accuracy results from refinements in areas of high stress gradients. For the sake of simplicity and economy, the models used in this study were refined only once and the element breakdown was uniform; no attempt was made to increase refinement in areas of expected high stress gradients. Each element of the original deck in both of the finite element models was quartered except for the two outside rows of deck elements, which were halved. The same refinement was applied to the web elements. Also, in both models the lengths of the beam elements were halved. The

corresponding response data from the refined models, namely displacements and stresses, were slightly larger, indicating a somewhat more flexible model. However, the largest of the variations was on the order of 3% and this was considered sufficiently insignificant that no further refinement was considered necessary.

Grillage Model

The initial representation of the span was in the form of a grillage model, which had the advantage of simplicity and which had previously provided satisfactory representations of slab structures. This model represented a single span of the bridge superstructure as a combination of longitudinal and transverse three-dimensional elastic beams. The layout of the grillage model used in this study, showing beam elements and nodes, is given in Figure 19. The model consisted of 32 longitudinal beam elements, 45 transverse beam elements, and 54 nodes. The longitudinal lines of nodes were located at the centerline of the girders and at the outer edges of the deck where the curb and railing were located.

The nine rows of transverse nodes were equally spaced along the length. This choice provided nodes at midspan, at the quarter points where the cover plates terminated, and at the eighth points. The midspan and quarter-point locations also corresponded to the location of strain gages and deflection gages. In addition, this particular nodal layout yielded longitudinal and transverse elements of almost equal length.

The properties of the longitudinal beam elements were determined from a cross section of the bridge span and were selected to represent the longitudinal girder and a portion of the concrete deck. For the exterior and interior longitudinal beam elements, the cross sections to be modeled are shown in Figure 20. For these elements, the slab sections were transformed to an equivalent steel section and the corresponding elment properties determined from the properties of the transformed cross section. The half depth of the beam element was chosen to be the distance from the neutral axis of the transformed section to the lower flange of the girder so that the predicted element stresses would correspond to the stresses measured during the experimental study.

In a similar manner, the transverse beam elements were selected to represent the transverse stiffness of the bridge deck, which was provided by only the slab. The properties of each transverse beam were calculated by considering equivalent properties of a transverse cross section of the deck as shown in Figure 21. Moments of inertia and area were calculated based on the gross concrete cross sections, and these values were used as the properties of the transverse beam elements.

The boundary conditions were first chosen to represent the idealized field support conditions as closely as possible. It was assumed that the slab prevented any significant rotation about the y- or x-axis (see Figure 19). Accordingly, all degrees of freedom at the nodes located along one support were constrained to zero with the exception of degree

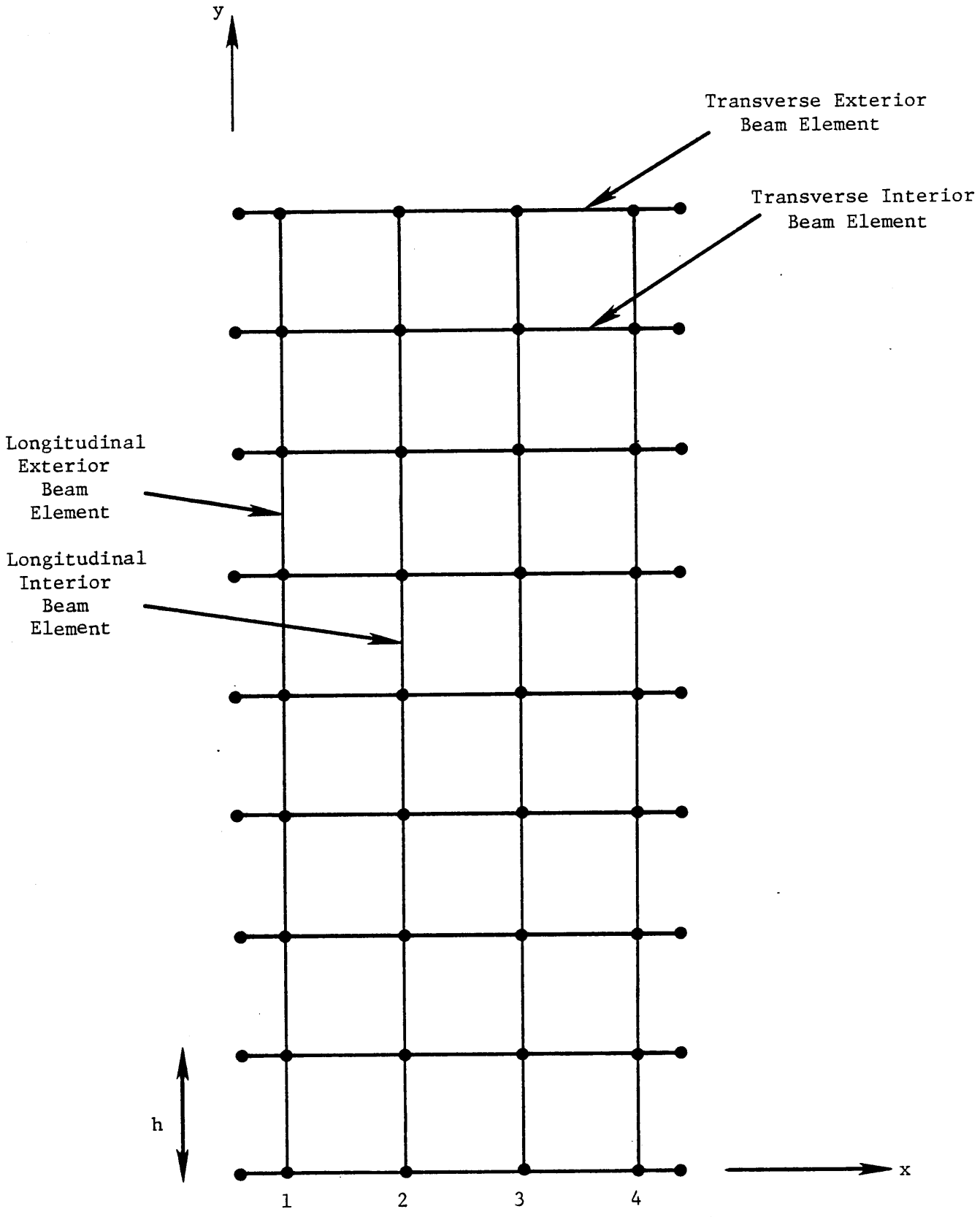

Figure 19. Plan view of the grillage model.

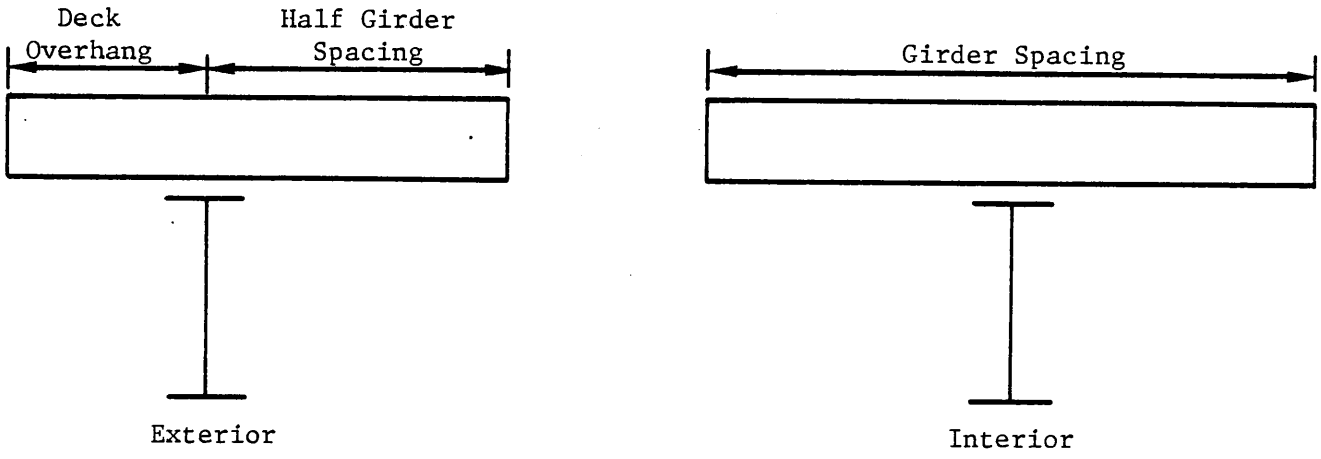

Figure 20. Longitudinal cross sections.

of freedom 4, rotation about the x-axis, which was unconstrained to represent an ideal pinned support. At the other support, degree of freedom 2, translation in the y-direction, was also unconstrained to simulate a roller support.

As will be noted in the subsequent discussion of results, the response of the grillage model was judged to be inferior to that of the finite element models in terms of being able to approximate the measured response. In addition, the modifications to the grillage model necessary to bring the predicted response in line the with measured response would have to be semi-rational at best, because of the approximations and assumptions already employed to represent a complex, three-dimensional structure as an assemblage of intersecting beams. Since the development and analysis of the finite element models entailed essentially no more effort and no more solution time, and since their response seemed to more accurately predict the actual response, no additional effort was spent on refinements and evaluation of the grillage approximation.

Beam/Slab Model

Two full finite element models of the bridge structure were developed in which both the slab and girders were represented by a combination of various types of finite elements. The only distinction between these two models was the manner in which the girders were represented. Both models used plate elements to represent the slab and either beam elements or a combination of beam and plate elements to

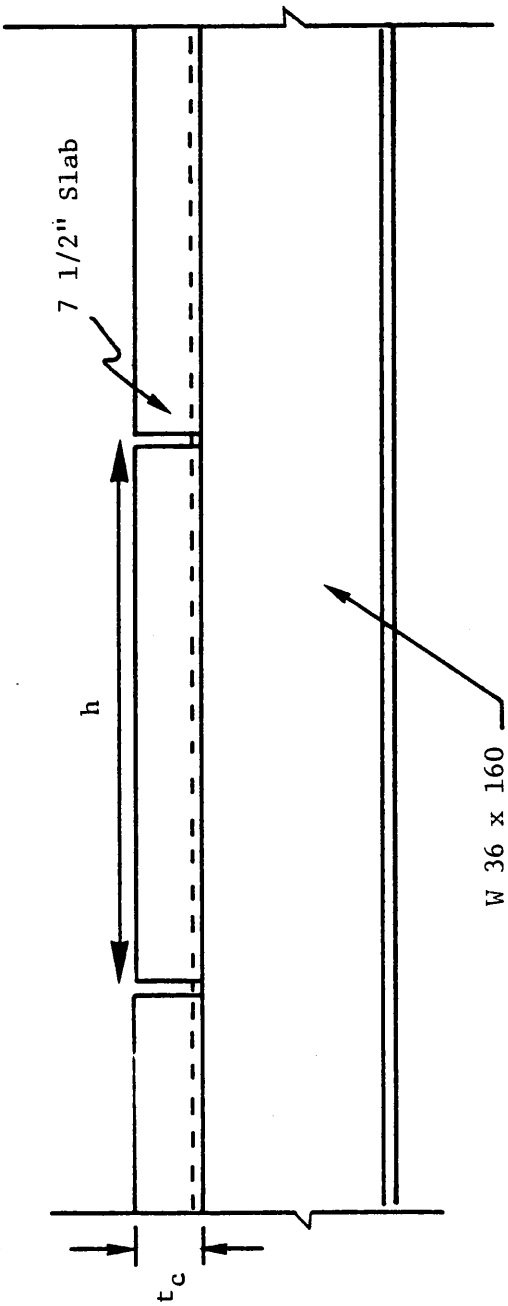

Figure 21. Transverse cross-section of bridge deck.

represent the girders. This type of model representation is a more logical and rational representation of the bridge span than is the grillage model, since each of the bridge components is modeled by elements that closely resemble the actual component.

The first finite element model developed was designated as a beam/slab model. In this configuration, the slab was represented by quadrilateral shell elements and three-dimensional beam elements were used to model the girders. Figure 22 is a plan view of the initial model layout showing the nodal locations, which were essentially identical to those selected for the grillage model. A schematic of the beam/slab model is provided in Figure 23. In this representative section, it is observed that the nodes of all shell elements were located at the centroid of the slab, while the nodes for the girder elements were located at the centroid of the girders. Coupling between the slab elements and girder elements was accomplished by prescribing coupling between the corresponding nodes. This coupling constraint, which essentially required two nodes with the same x-y coordinates to undergo identical displacements, was intended to simulate composite action between the slab and the girders.

Proper coupling between the upper set of nodes in the slab and the lower plane of nodes connecting the beam elements should, theoretically, represent the actual behavior of the girder/slab assembly. However, the coupling capabilities available in the several computer codes used in this study were unable to define the unique type of coupling required to adequately describe composite behavior. This shortcoming of the computer codes resulted in models which were far too flexible in the longitudinal direction. Because of the coupling difficulties, the model was subsequently modified to better represent the composite behavior of the slab/girder system.

In the second version of this model, the beam elements were modified such that all nodes were in the same plane; thus, the centroids of the beam elements were in the same plane as the centroids of the plate elements representing the slab, as shown in Figure 24. This arrangement eliminated any coupling problems, but required careful and rational derivation of the beam element properties to ensure that the final beam/slab model was a realistic representation of the actual structure.

The dimensions of the shell elements were chosen to correspond to the gross dimensions of the slab section each represented and the material properties chosen to be those of the concrete in the slab. The geometry and dimensions of the longitudinal beam elements were chosen in such a way that their properties -- namely area, centroid, depth, and moments of inertia -- would be identical to the properties of the actual composite cross section. These properties were chosen in the following manner. The cross section to be modeled by the longitudinal beam elements was to consist of a girder and a portion of the slab. The properties of the corresponding transformed section of this girder/slab configuration were calculated and an equivalent cross section having

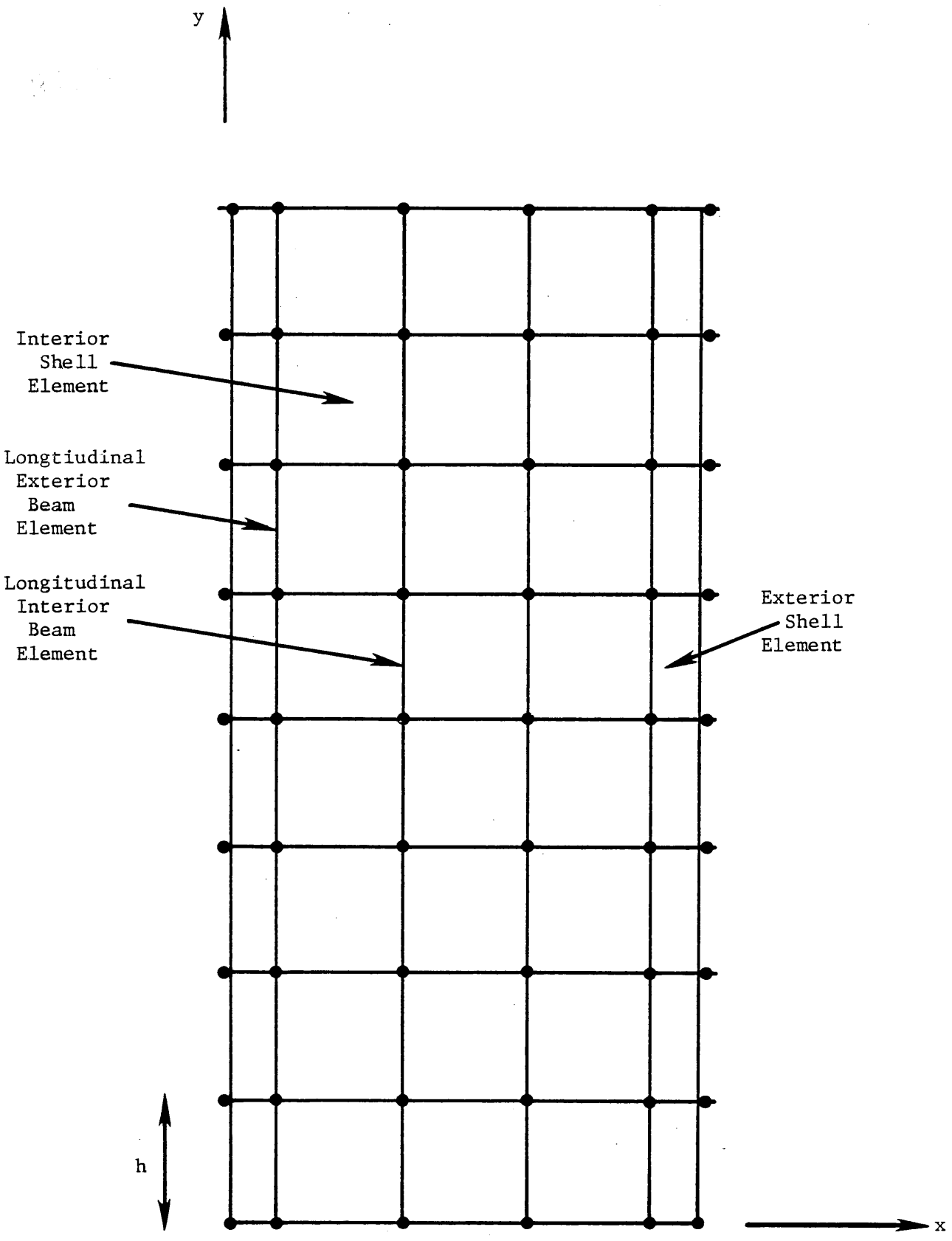

Figure 22. Plan view of beam/slab model.

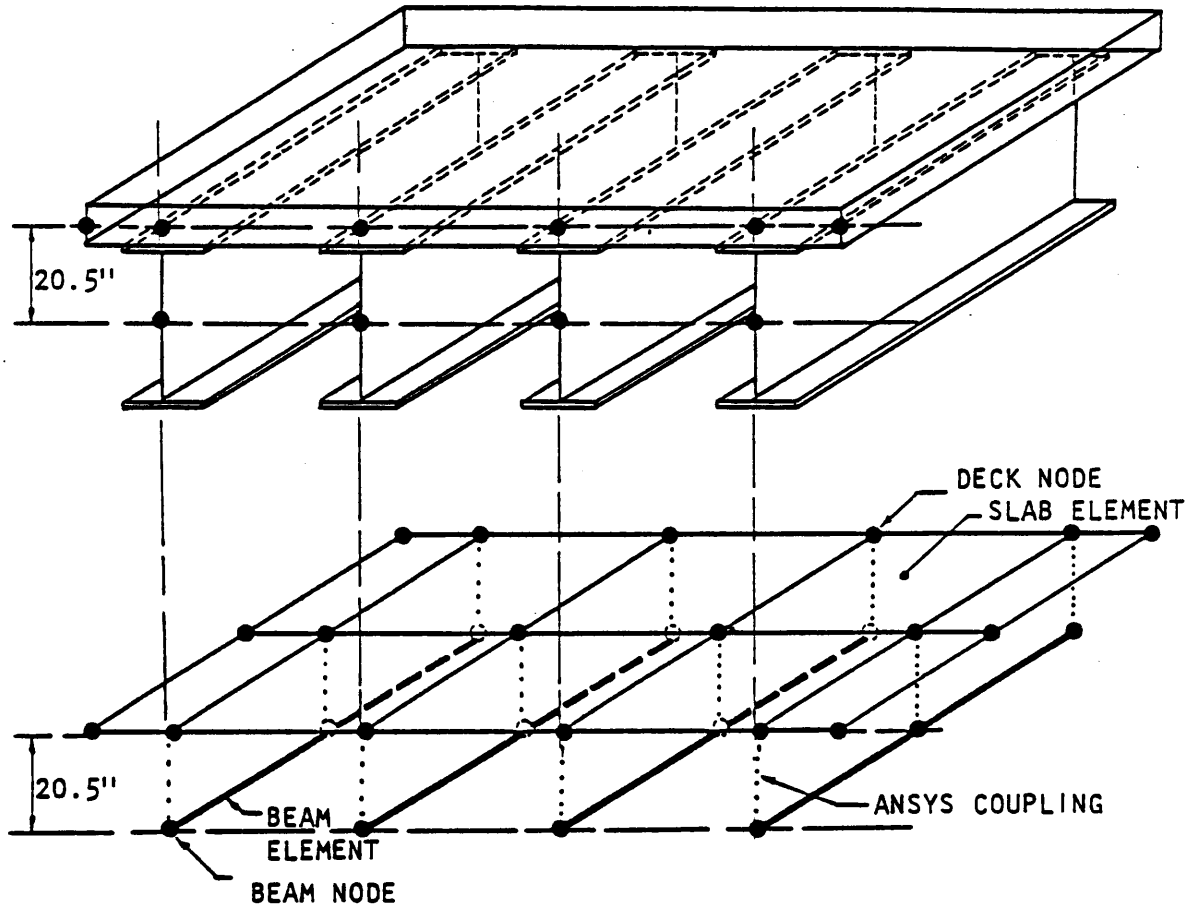

Figure 23. Schematic of beam/slab model.

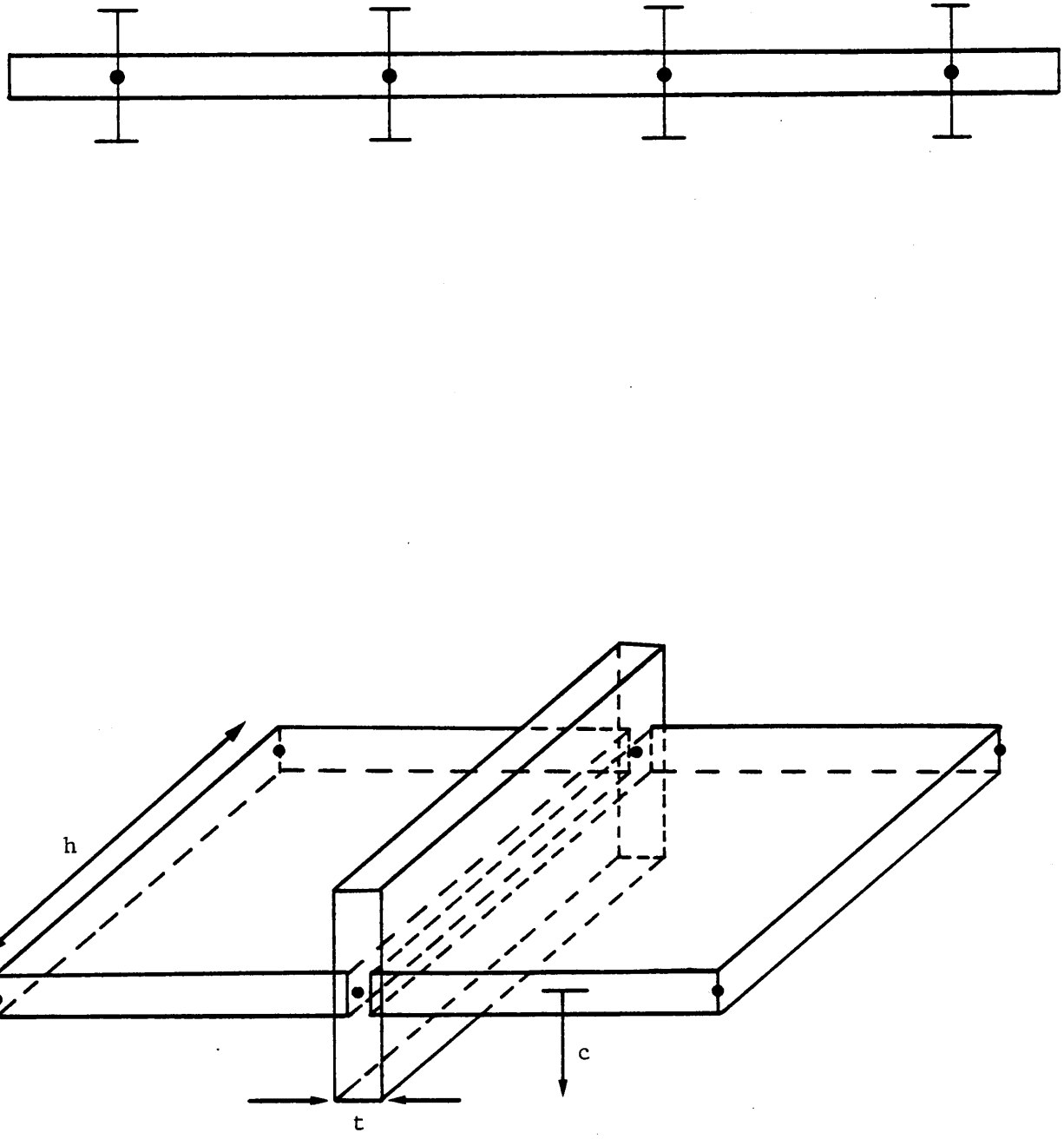

Figure 24. Modified beam/slab model with all nodes in same plane.

essentially the same properties was chosen for the beam elements. The moment of inertia was the only property that was modified, and that was reduced by an amount equal to the moment of inertia contributed by the slab elements. With this choice of properties, the composite action was modelled reasonably accurately. The predicted stresses corresponded to those measured on the lower flange, since the element depth was chosen to match the distance from the neutral axis to the lower flange, and thus the predicted response based on the model could be easily compared with the measured experimental response.

A sketch of the final beam/slab computer model is shown in Figure 25. This model, as was true for all analytical models in this study, did not include transverse stiffness or curb/railing effects. The boundary conditions imposed were the same as those used for the grillage model; namely, pinned support along one edge and roller supports along the other boundary. The effect of different boundary conditions, or different degrees of continuity, were extensively evaluated, however, and these effects are presented and discussed in the subsequent section on results.

While this model was judged to be a logical and rational representation of the actual bridge span and was capable of incorporating and evaluating a number of parameters, the representation of the girders obviously involved some approximation. To gain further understanding of the effects of this approximation, and to investigate whether a better representation of the girder would result in an overall improved finite element model, another model of the bridge was developed.

Plate/Slab Model

In the development of the beam/slab model described in the previous section, an equivalent beam was used to model the girders wherein the portion of the stiffness properties of the composite section allocated to the beam necessarily involved assumptions and approximations. To eliminate the uncertainties involved in the use of an equivalent beam to model the girders, a more refined finite element model was developed and investigated. In this model, the slab was again modelled using quadrilateral shell elements, but the girders were modeled using plate elements to represent the web of the girders and beam elements to represent the upper and lower flanges. In this particular modelling scheme, the actual geometry and properties of the girder could be more accurately represented with the centroid of the girder model located at the actual girder centroid. A sketch of this model, which will be referred to as the plate/slab model, is shown in Figure 26.

The same nodal layout used in the previous models was retained in the plate/slab model. Each girder segment was modelled using three elements -- two beam elements and one plate or plane stress element. Thus, the plate/slab model consisted of 90 nodes, 40 quadrilateral shell elements (slab), 32 plane stress elements (web), and 64 three-dimensional beam elements (flange). As shown in Figure 26, the nodes for the deck elements, the upper flange elements, and the top edge of the web elements

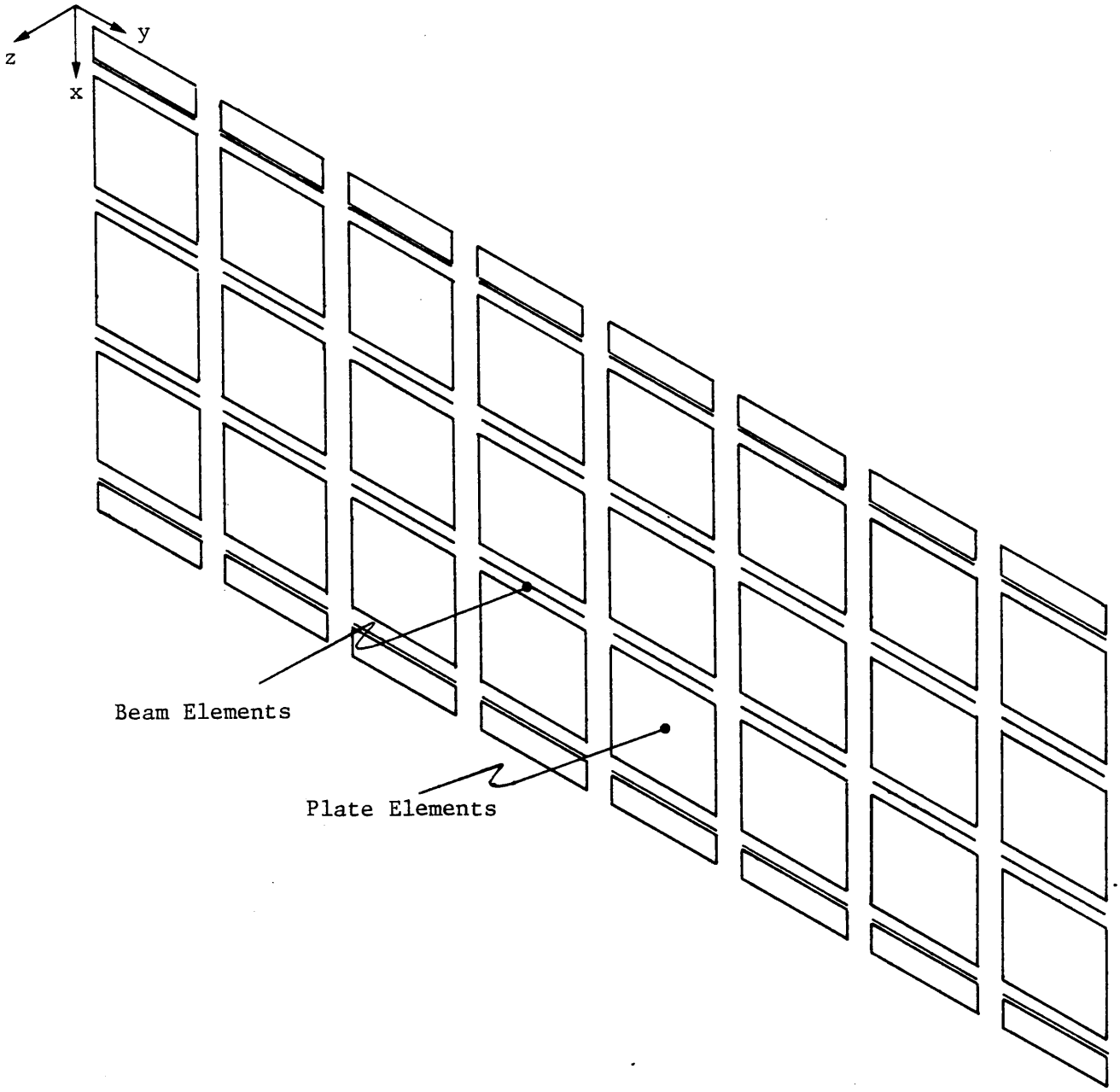

Figure 25. Final Beam/Slab Model.

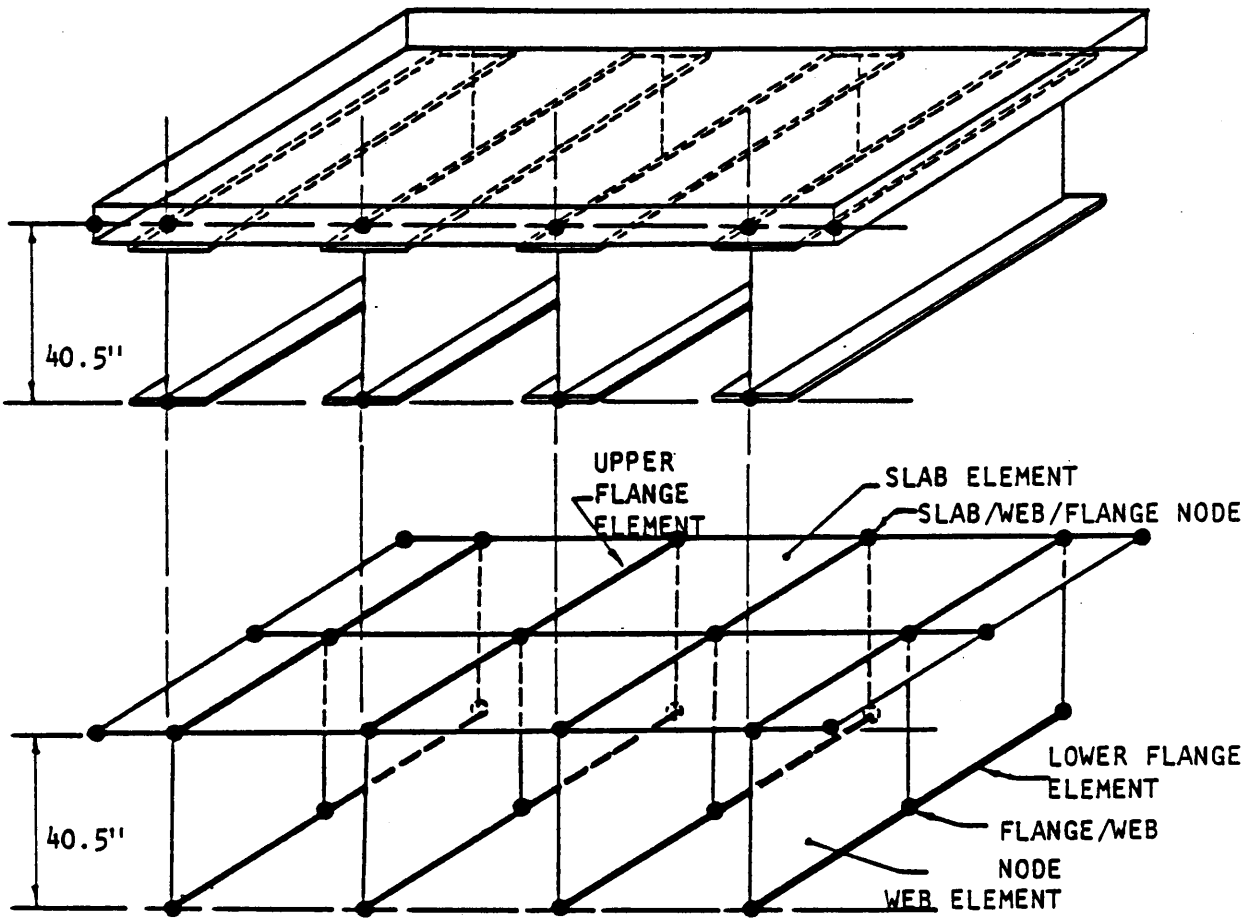

Figure 26. Schematic of plate/slab model.

were all located in the same plane. The fact that the upper flange of the girder was at the bottom of the slab rather than the centroid meant that the depth of the girder in the model was somewhat larger than the actual depth. To maintain the same effective moment of inertia, the area of the beam element representing the upper flange was simply reduced.

Another sketch of the computer-generated plate/slab model is shown in Figure 27. The plate/slab model has 90 nodes in a three-dimensional array with 380 degrees of freedom, while the beam/slab model has only 54 nodes in a two-dimensional array with 228 degrees of freedom. This plate/slab model, for the same general nodal layout, is thus a more complex model of the bridge than is the beam/slab model. However, as will be shown, although the basic plate/slab model yields deflections and stresses more closely approximating measured responses, the simpler beam/slab model does an adequate job and can, in fact, be modified in such a way that its predicted response is almost identical to that measured in the field. The final choice of a particular analytical model will likely depend on a number of factors, including available software, type of computer available, and personal preferences of the analyst.

Model Modification

As noted earlier, of all model parameters examined, only support continuity and inclusion of the curb/railing had any significant effect on model response, at least if the range of parameter variations were limited to realistic and practical values. Accordingly, the manner in which these factors were incorporated in the models is described in some detail in the following sections.

Curb/Railing

In the analysis and design of typical bridge structures, the walkways, parapets, and railings are not considered to be structural, load-carrying elements. Consequently, in the initial development of the two finite element models, the curb and railing were not included. However, if the curb/railing does act integrally with the slab, there is the possibility that it can significantly influence the behavior of the bridge. In the bridge used in this study, as is typical with most bridges of this type, some composite action between the railing and deck was provided by shear keys in the form of reinforcing bars extending from the deck into the cast-in-place railing.

Determining the precise degree of interaction between deck and railing is difficult, but for purposes of this study two cases were examined. These were the fully composite interaction between deck and railing and the noncomposite case where the deck and railing act totally independently. The idealized cross section of the curb/railing and that portion of the deck assumed to act with the exterior girder is shown in Figure 28. For both the composite and noncomposite cases, neutral axis

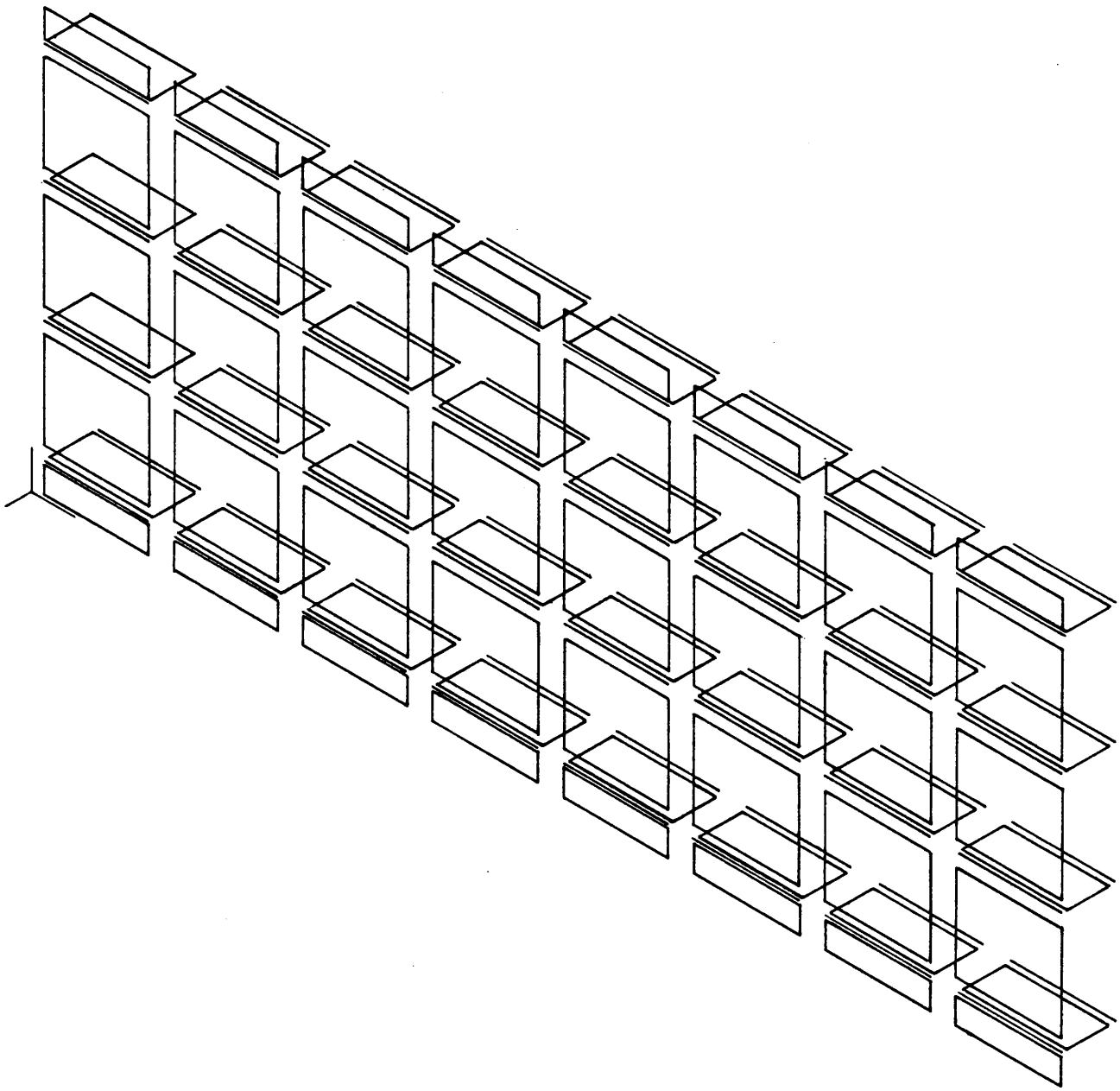

Figure 27. Final plate/slab model.

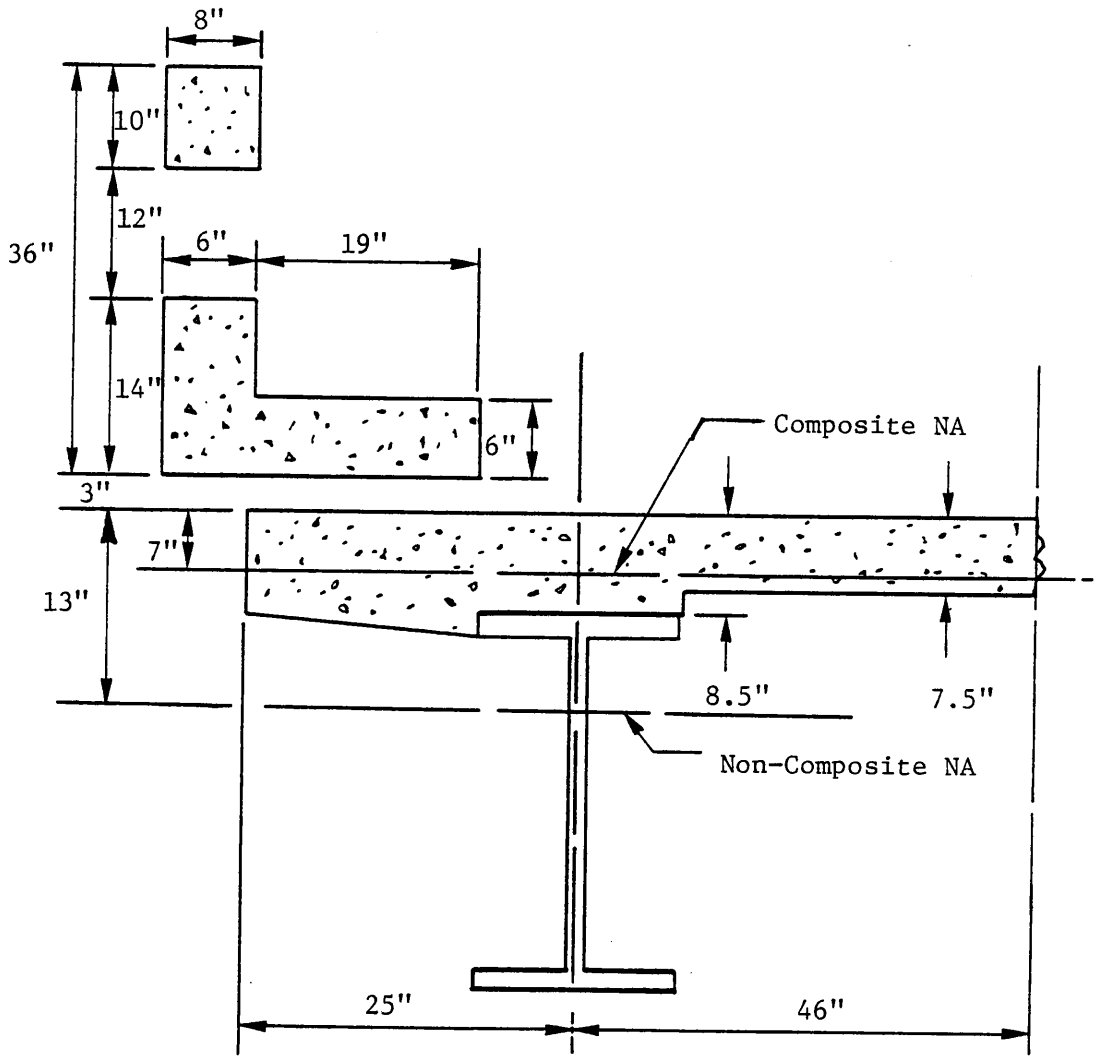

Figure 28. Cross-section of curb/railing.

locations were determined, as indicated in Figure 28, and corresponding values of stiffness were calculated for the curb/railing portion of the structure. Beam elements with these properties were then added to the beam/slab and plate/slab finite element models to simulate the effect of the curb/railing on the bridge response.

Support Continuity

As discussed in the earlier section on "Test Results", the experimental data indicated the existence of some continuity at the supports. Since the instrumentation was not designed specifically to investigate continuity, the precise degree of rotational constraint could not be identified, but it was estimated that the restraint would be not less than 10% nor more than approximately 25%. Accordingly, modifications were made to the models to reflect some degree of rotational restraint at the supports, with the degree of restraint adjusted to at least approximate that indicated by test data.

There are a number of ways partial fixity or continuity can be incorporated into finite element models of a bridge span. To some extent, the choice of a particular scheme is dependent on the finite element code available and whether or not the code will accept certain modifications such as rotational spring elements. In this study, three techniques were considered for including the effect of continuity and partial fixity at the supports.

The first approach was to add rotational spring elements at the boundary nodes and adjust the spring stiffness to correspond to the degree of fixity desired. Although spring elements are available in some codes (e.g. ANSYS), they were not available in all of the computer codes used in this study and, consequently, two alternative schemes were also utilized.

The effect of a rotational restraint can also be simulated by adding three-dimensional beam elements attached at the boundary nodes and extending beyond the boundary point. The effective rotational stiffness can be prescribed by appropriate selection of the parameters E, I, and L. This procedure of introducing support continuity was utilized in both the beam/slab and plate/slab models.

A final, convenient method of restraining rotation at the boundary nodes is to prescribe a moment reaction at the nodes where the magnitude of the applied moment is selected as a percentage of the fixed-end moment developed for the particular loading applied.

While any of the three methods for representing support continuity/fixity can be used, with a proper assignment of parameters, to yield satisfactory results, each has certain undesirable features. For example, the use of spring elements is possible only with certain codes although, where possible, it is likely the most convenient procedure. The use of dummy beams to represent adjacent spans increases the number

of elements and nodes, although this approach seems physically rational and is intuitively appealing. And the application of end moments to represent partial fixity is a convenient and rational scheme but first requires the determination of fixed-end moments (complete fixity) for each loading condition.

Based on results from models incorporating continuity/fixity to be presented subsequently, each of the three techniques for modeling fixity produced essentially identical effects on response, and the choice of a particular method depends only on the preference of the analyst and the computer code available for use.

Loadings

As noted previously, the test vehicle used to load the bridge in the field test was a three-axle dump truck filled with gravel to obtain a gross total weight of 57.22 kips. The axle spacings, wheel locations, and loads were shown in the sketch in Figure 13.

In the experimental study, 25 load positions of the test vehicle were used. However, it was neither practical nor necessary to include all of these load cases in the analytical study. For example, gage sections 2 and 3 located only inches apart at the end of the cover plate in span B yielded essentially the same results. Gage sections 1 and 4 were both midspan locations, but in adjacent spans in the experimental study. Symmetry considerations, both longitudinal and transverse, not utilized in the experimental program, also can be used to significantly reduce the number of different load cases. Based on all of these considerations, only six independent load positions needed to be considered. Based on preliminary studies and response data, four load cases were chosen for detailed analysis and are the ones referred to in the subsequent discussion and comparison of results. The four load cases selected for use in the analytical study were equivalent to load case 3-4 (centerline/midspan), load case 1-4 (curb/midspan), load case 3-2 (centerline/quarter point) and load case 1-2 (curb/quarter point). For each of these loadings, it was necessary to develop equivalent nodal loads for use with the finite element models.

Two procedures were employed to obtain the equivalent nodal loadings loadings from the actual wheel position locations. First, for each load case, the interior wheel loads on a deck element were transformed to nodal loads by using the relatively simple shape functions of the classical 12 degree of freedom plate bending element to define these nodal loads. However, relatively few modern finite element codes actually use this first-generation bending element; although the loads derived in this manner were considered satisfactory, a second technique was also considered. Using this alternative scheme, an analysis was conducted of a single plate element, fixed at all nodes, and loaded with the actual wheel loads whose locations corresponded to the particular load case. The resulting nodal reactions were then used as the

equivalent nodal loads in the full finite element analysis of the bridge span. Although this procedure required a separate analysis of each loaded element for each load case, it could be used with all computer codes employed and certainly yielded reliable nodal loads. Consequently, this latter procedure was used for generating loads for all analyses presented in this section.

Computer Codes

Three large-scale finite element codes were employed for the analysis of the finite element models. These three codes, namely SAP IV, SPAR, and ANSYS, were readily available and familiar to the investigators and were included to evaluate ease of use and modelling capability, and to ensure consistency of response prediction. As would be expected, all codes provided essentially the same response information, but the various features and capabilities of the three codes did differ somewhat.

The SAP IV code (2), originally developed at the University of California, was the oldest of the three codes used and consequently was more limited in several respects. The version used in this study had only 6 element types in its library. All input was formatted, somewhat of an inconvenience, and there was no output control. Also, prescribing constraints and coupling was more limited than with the other codes. Nevertheless, it is a widely available and widely used code and, although more inconvenient than some others to use, can still adequately analyze the finite element bridge models developed in this study.

The SPAR program (3) was developed under contract to NASA and the version used in this study was made available in 1978. It has an element library of some 18 element types and more versatile input and output options than SAP IV. Its complete problem definition, including constraint and coupling features, was much simpler than that required by SAP IV but still somewhat cumbersome.

The ANSYS program (4), developed by Swanson Analysis Systems, Inc., is one of the more widely used commerical codes and consequently is being continuously modified and upgraded. The version of ANSYS used in this study is Release 4.0, revised in 1983. It is one of the most comprehensive codes available containing 95 element types and capable of dynamic and nonlinear analyses in addition to static analysis. Because of its wide commercial application, it has been made particularly easy to use considering its capabilities.

Since all codes produced essentially the same response information, and since ANSYS was the code with the most capability in analysis and in postprocessing, ANSYS was selected for use in all of the analyses presented in this report.

Analytical Results

The results discussed in this section are based on the response predicted by the two finite element representations of the bridge; namely, the beam/slab and the plate/slab models. While all six load cases were analyzed, only the results from four load cases are presented, and of these only the selected response information will be discussed. Response data from the basic finite element models are presented, as well as results from these models modified to include support continuity/fixity and curb/railing effects. It was not feasible to include a discussion of the predicted stresses and deflections at all points corresponding to those where experimental data were measured during the field test because of the large amount of data.

The response data probably most indicative of the characteristic behavior of the bridge and most useful for comparison with measured experimental responses were the deflections and lower flange (maximum) stresses at the quarter point and at midspan. Accordingly, these response data are the ones primarily used for evaluating the analytical models and for comparing predicted and measured stress and deflection values. Also, for convenience in discussion, analytical results from the various models are first presented and discussed separately and then compared and evaluated.

Beam/Slab Model Results

The beam/slab model was subjected to the four load cases previously described, and stress and displacement data at all nodal locations were calculated. These data included specifically the vertical deflections and lower flange longitudinal stresses in addition to nodal rotations, longitudinal and transverse displacement, and stresses in the slab. As was noted earlier, stresses corresponding to those in the lower flanges of the girders were generated by choosing the beam elements representing the girders to have a depth equal to twice the distance from the neutral axis of the composite girder/slab to the lower flange. For all load cases discussed in this section, ideal simple supports were assumed and no effect of the curb/railing was included.

Load case 3-4 corresponded to the test vehicle in the centerline of the bridge at midspan, load case 1-4 corresponded to the vehicle in the curb lane at midspan, and load case 3-2 corresponded to the test vehicle in the centerline lane at the quarter point of the span. These three load cases were selected as representative of all loadings for the evaluation of the beam/slab model. Values of displacements and stresses for these loadings are tabulated in Tables 9 and 10, and plots of the transverse distribution of displacements and stresses at the quarter point and midspan are presented in Figures 29 through 34. Also plotted in these figures are the corresponding experimental data determined from the field tests. Although the characteristics of the deflection and stress data distribution are similar, it is believed that the deflection data are a better basis for comparison and evaluation purposes.

TABLE 9

Displacements for the Beam/Slab Model, in

Load Case	Girder 1	2	3	4
		At Quarter Point		
3-4	0.081	0.134	0.133	0.080
1-4	0.001	0.064	0.148	0.224
3-2	0.069	0.128	0.127	0.068
		At Midspan		
3-4	0.114	0.195	0.195	0.113
1-4	0.001	0.090	0.215	0.323
3-2	0.094	0.156	0.155	0.092

TABLE 10

Maximum Stresses for the Beam/Slab Model, psi

Load Case	Girder 1	2	3	4
		At Quarter Point		
3-4	1,220	1.745	1,744	1,211
1-4	24	1,011	2,013	2,953
3-2	1,127	2,800	2,794	1,108
		At Midspan		
3-4	1,529	3,030	3,024	1,511
1-4	13	1,272	3,404	4,731
3-2	1,273	2,129	2,110	1,240

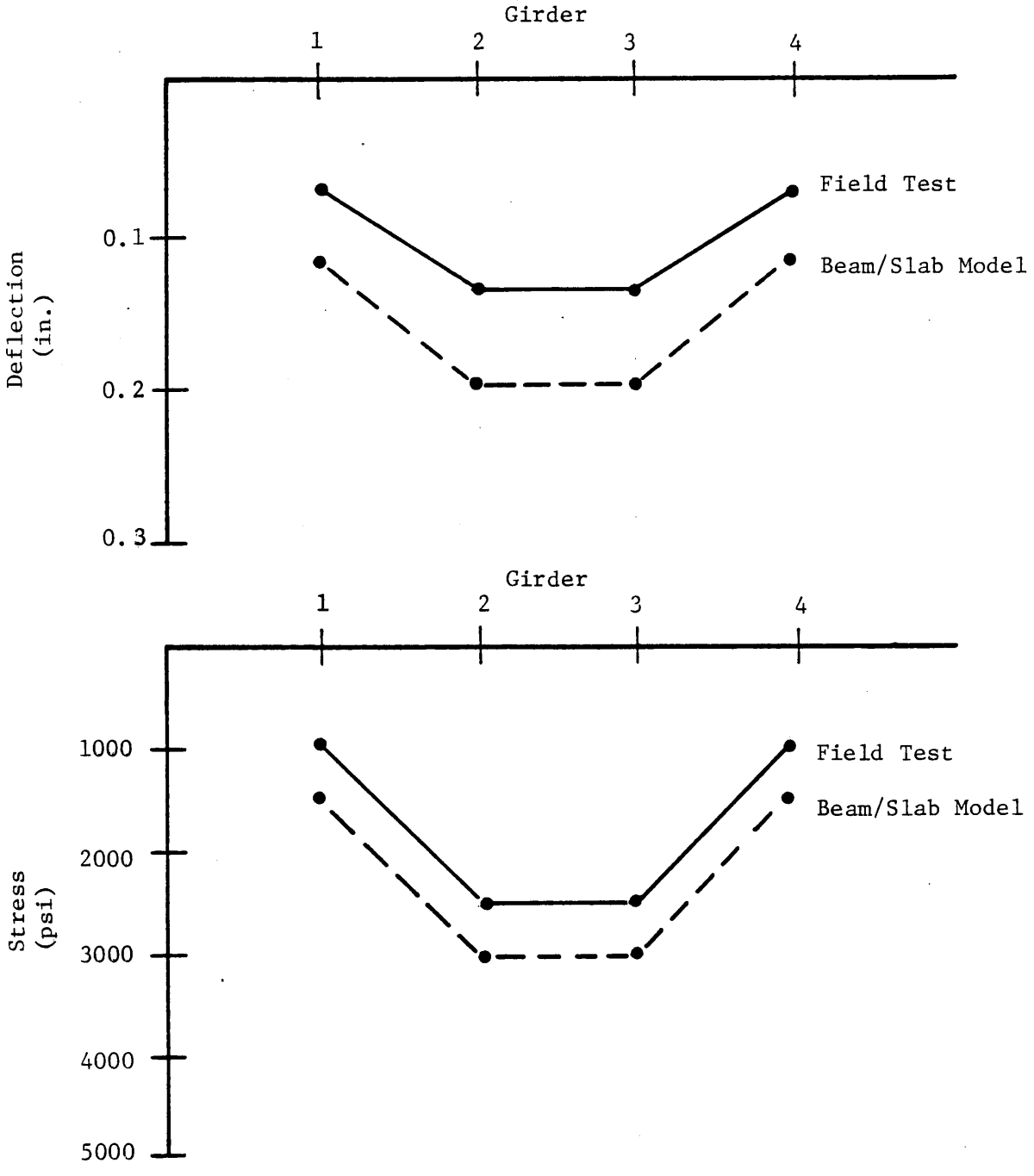

Figure 29. Plot of displacement and maximum stress at midspan -- Load Case 3-4.

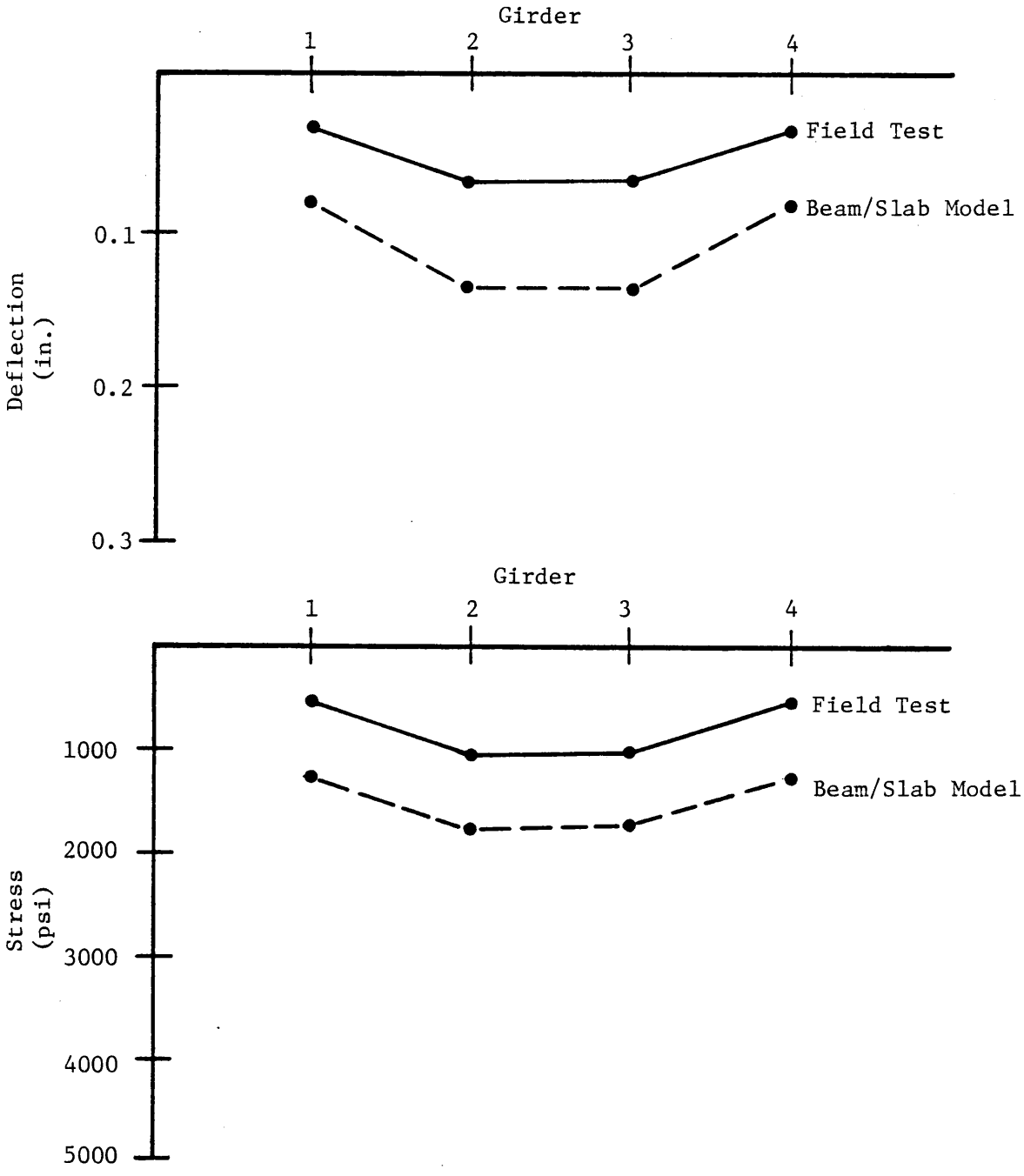

Figure 30. Plot of displacement and maximum stress at quarter point -- Load Case 3-4.

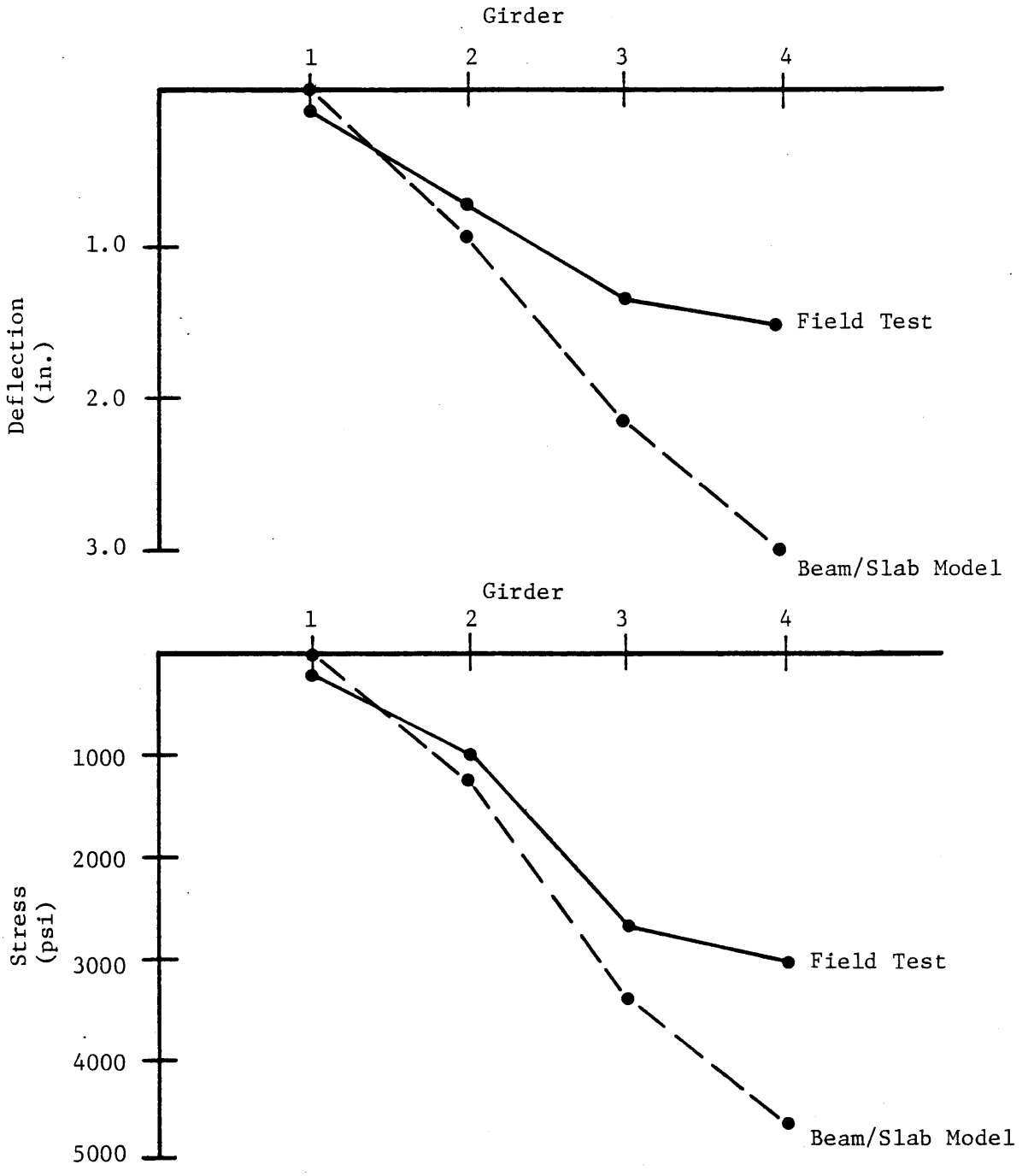

Figure 31. Plot of displacement and maximum stress at midspan -- Load Case 1-4.

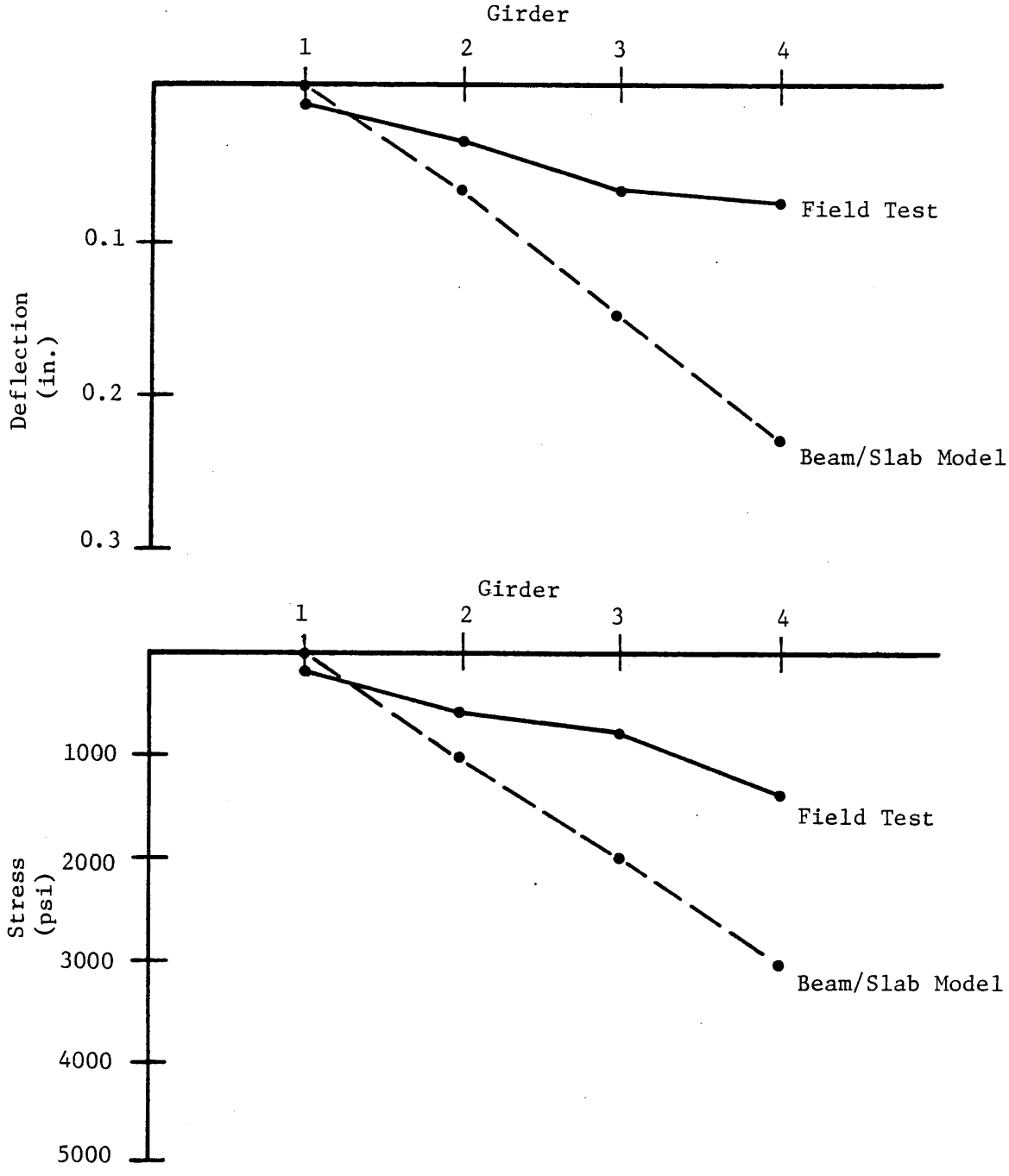

Figure 32. Plot of displacement and maximum stress at quarter point -- Load Case 1-4.

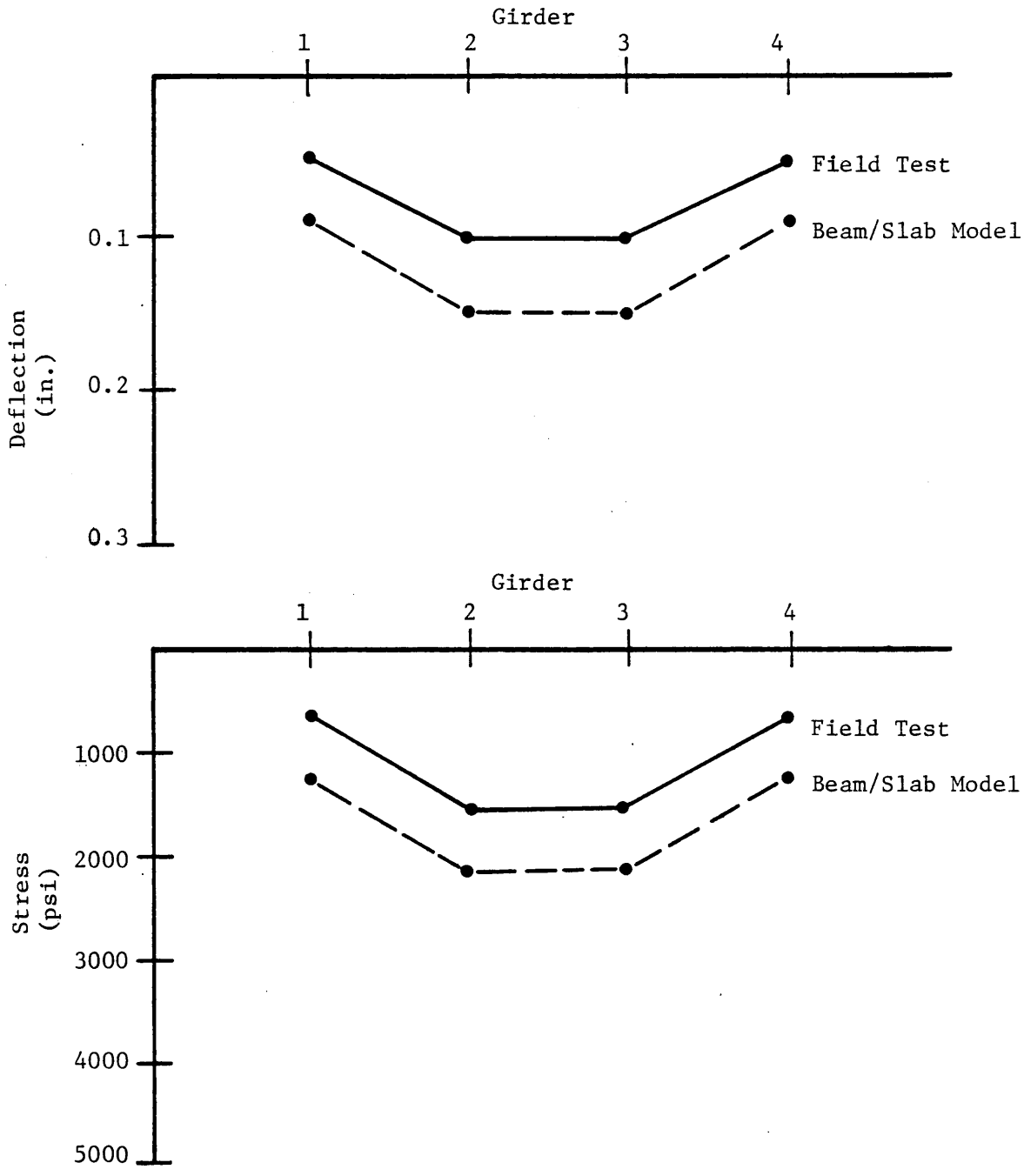

Figure 33. Plot of displacement and maximum stress at midspan -- Load Case 3-2.

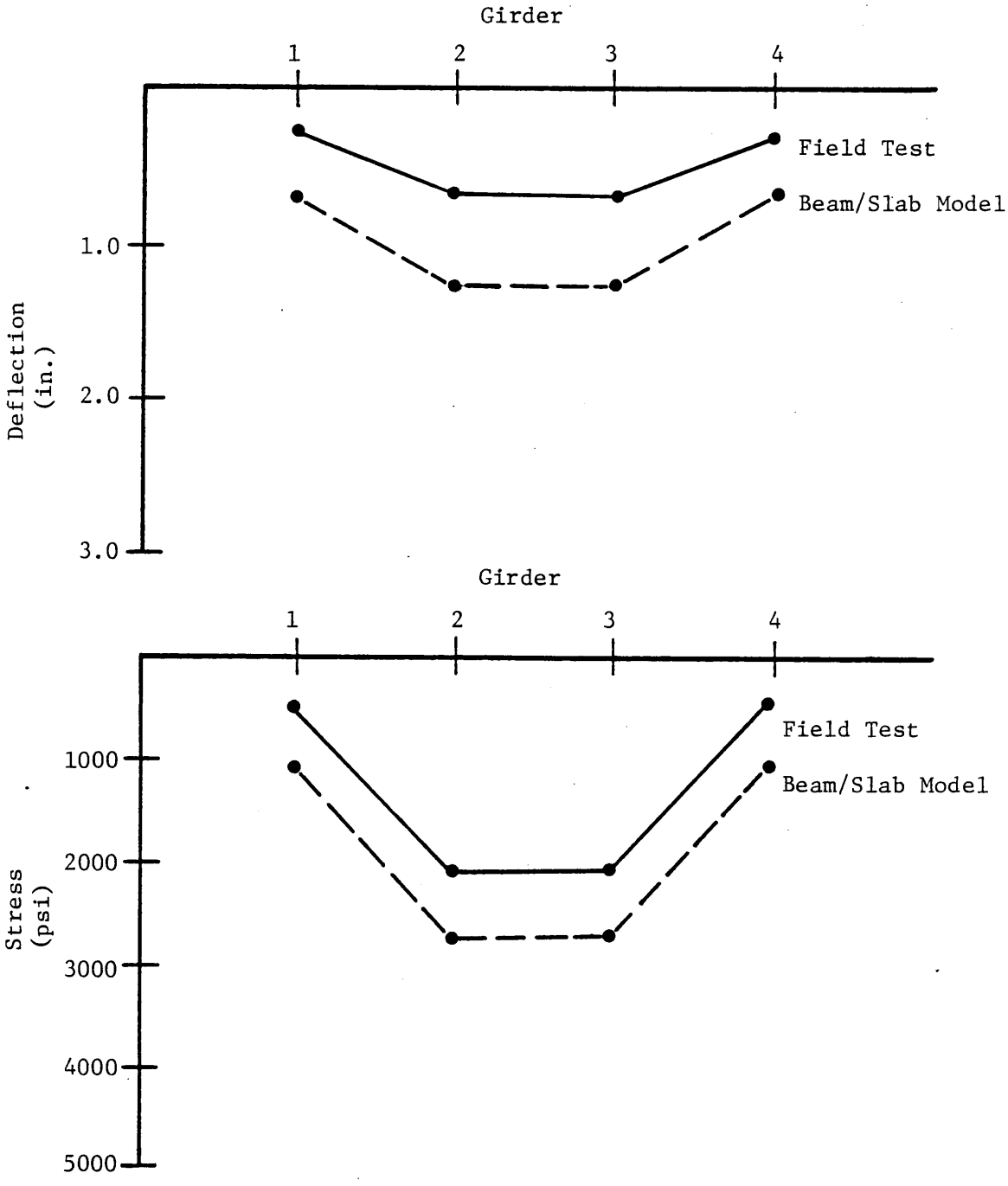

Figure 34. Plot of displacement and maximum stress at quarter point -- Load Case 3-2.

From the data it may be observed that the general shapes of the predicted and measured transverse distributions of stress and deflection are similar, although the values of predicted and measured quantitites differ significantly. This would seem to indicate that the model representation of the transverse stiffness were reasonably accurate, but the longitudinal stiffness of the model was considerably less than that of the bridge. For example, under load case 3-4 the maximum deflection at midspan predicted by the model was approximately 0.20 in, while that measured experimentally was 0.13 in, a difference of approximately 50%. Variations between predicted and measured deflections at the quarter point were even larger, as shown in Figure 30. From Figures 31 and 32, which are the response data resulting from load case 1-4 with the test vehicle at midspan in the curb lane, the stresses and deflections varied from essentially zero at the girder farthest from the load to a maximum at the loaded edge. It may be recalled that with the test vehicle in the curb lane or lane 1, the wheel lines were almost exactly over the two outermost girders (see Figure 14). Thus, it would be expected that the maximum stresses and deflections would be produced with the vehicle in the curb lane at midspan. This is, in fact, what was observed for both the analytical and experimental values. For example, the maximum deflections at midspan for load case 1-4 were 0.323 in from the model and 0.148 in from the experimental data. Corresponding values of lower flange stress were 4,730 psi and 2,950 psi, respectively.

Although the response data from this model did not indicate an obvious need for the addition of curb/railing, it was considered desirable to examine this factor and its effect on the responses. In this case, it was assumed that the curb/railing was not composite with the deck, and additional beams with an equivalent stiffness were simply added along the exterior edges of the model.

The effect of adding the curb/railing stiffness to the beam/slab model is shown in the response data in Figures 35 and 36. Based on these data and similar data calculated at other points, it was concluded that the effect of curb/railing on the overall deflection and stress response was relatively insignificant. Accordingly, this parameter was not included in subsequent analyses using the beam/slab model.

A more significant parameter was that of support conditions; thus the addition of a model parameter that would simulate some degree of fixity or continuity at the supports was essential. As was discussed previously, the experimental data indicated that the degree of fixity, as determined from deflections measured in a span adjacent to the loaded span, was on the order of 10% to 12%. The beam/slab model was modified by adding dummy beams as extensions of the girders in adjacent spans to simulate continuity. The values of E, I and L for these dummy beams were chosen such that the degree of fixity was approximately 12 percent. This modified system was considered to be the best representation of the bridge that could be achieved within the constraints of the size and type of model developed.

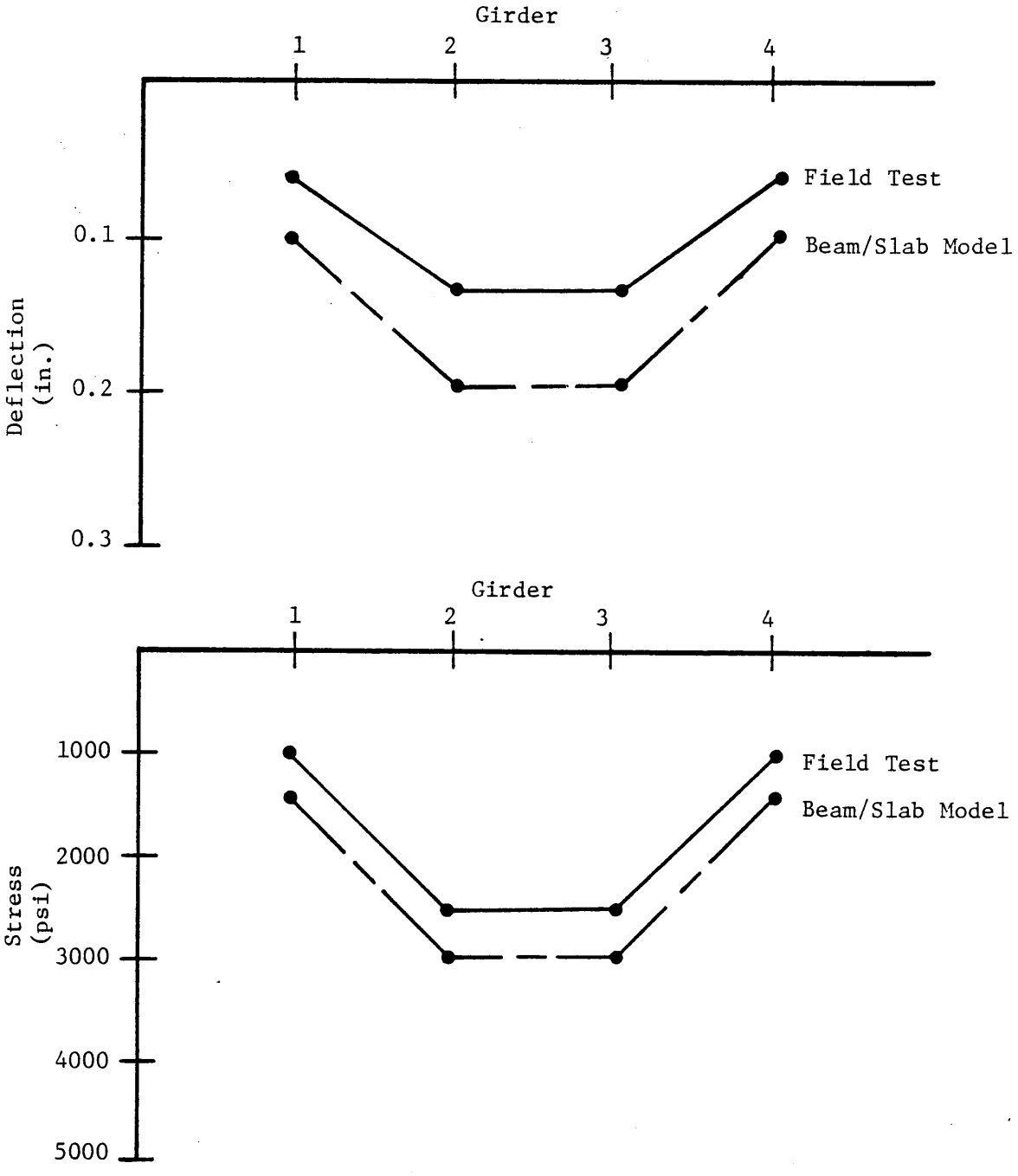

Figure 35. Plot of displacement and maximum stress at midspan -- Curb/Railing included -- Load Case 3-4.

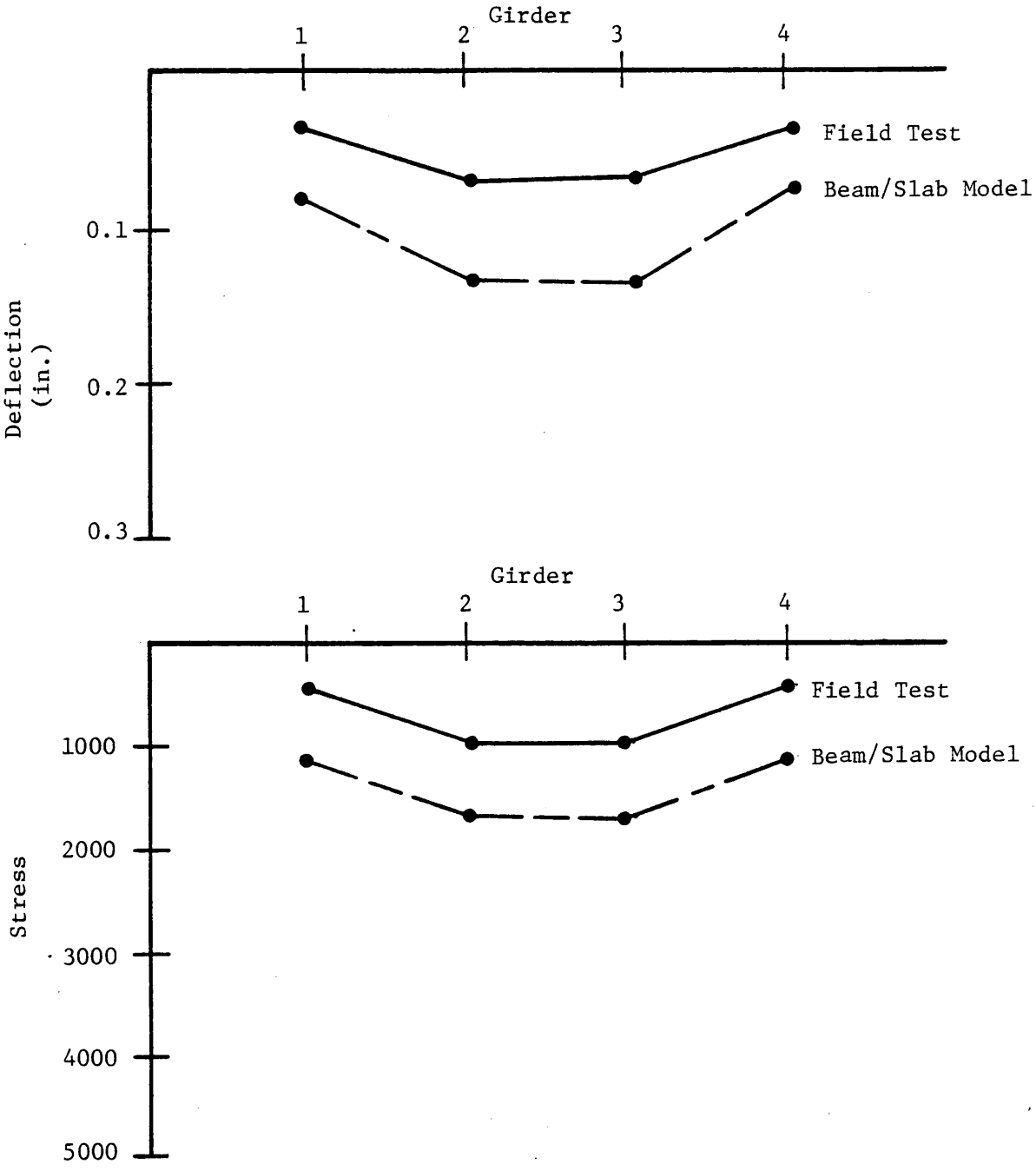

Figure 36. Plot of displacement and maximum stress at quarter point -- Curb/Railing included -- Load Case 3-2.

This final bridge model was reanalyzed under load cases 3-4, 1-4, and 3-2, and the predicted deflection and stress data at midspan and at the quarter point for these three load cases are plotted in Figures 37 through 42. For comparison purposes the corresponding experimental values of deflection and stress are plotted in the same figures. The first observation is that the predicted values of stress and deflection compared very favorably with those measured in the field test. For example, at midspan under load case 3-4, which produced the maximum response, the predicted deflection were within approximately 5% of the corresponding experimental value and the predicted stress within 10%. For this particular loading, the predicted stresses and deflections were slightly less than the experimental values at midspan and slightly larger at the quarter points. In fact, this same trend seemed to hold for all load cases. It is also of interest to note that the wide discrepancy between the experimental data and the response predicted by the beam/slab model without continuity for load case 1-4 has been corrected and the agreement between the analytical and experimental values is now quite favorable as seen in Figures 39 and 40.

Comparisons of the experimental responses and those predicted by the modified beam/slab model were made for several additional load cases, and these data were also found to compare favorably.

Plate/Slab Model Results

As described in the previous section, the plate/slab model was intended to provide a somewhat more realistic representation of the actual structure than the beam/slab model by modelling the girders using beam elements as the flanges and plate elements for the web. Other than the girder representation, all other aspects of the beam/slab and plate/slab models were the same. Unless otherwise noted, the results presented are for the basic plate/slab model with simple supports at both ends and with the curb/railing not included. Although the plate/slab model had almost twice as many nodes, and hence twice as many degrees of freedom, the primary response data used for evaluating and comparing the model were vertical deflections at nodes along the lower flange and maximum stresses, which also occurred at the lower flange nodes. The plate/slab model was analyzed for all six independent load cases. However, for convenience, most of the results discussed in this section will be for one symmetrical or centerline loading at midspan, load case 3-4, and one nonsymmetrical or curb loading at the quarter point, load case 1-2.

Values of displacements and stresses at quarter point and midspan transverse sections for load cases 3-4 and 1-2 are presented in Table 11, and plots of the transverse distribution of deflections and stresses at the quarter point and midspan are shown in Figure 43 through 46. Clearly, this analytical model was again more flexible than the actual structure based on comparisons of the predicted and measured deflections.

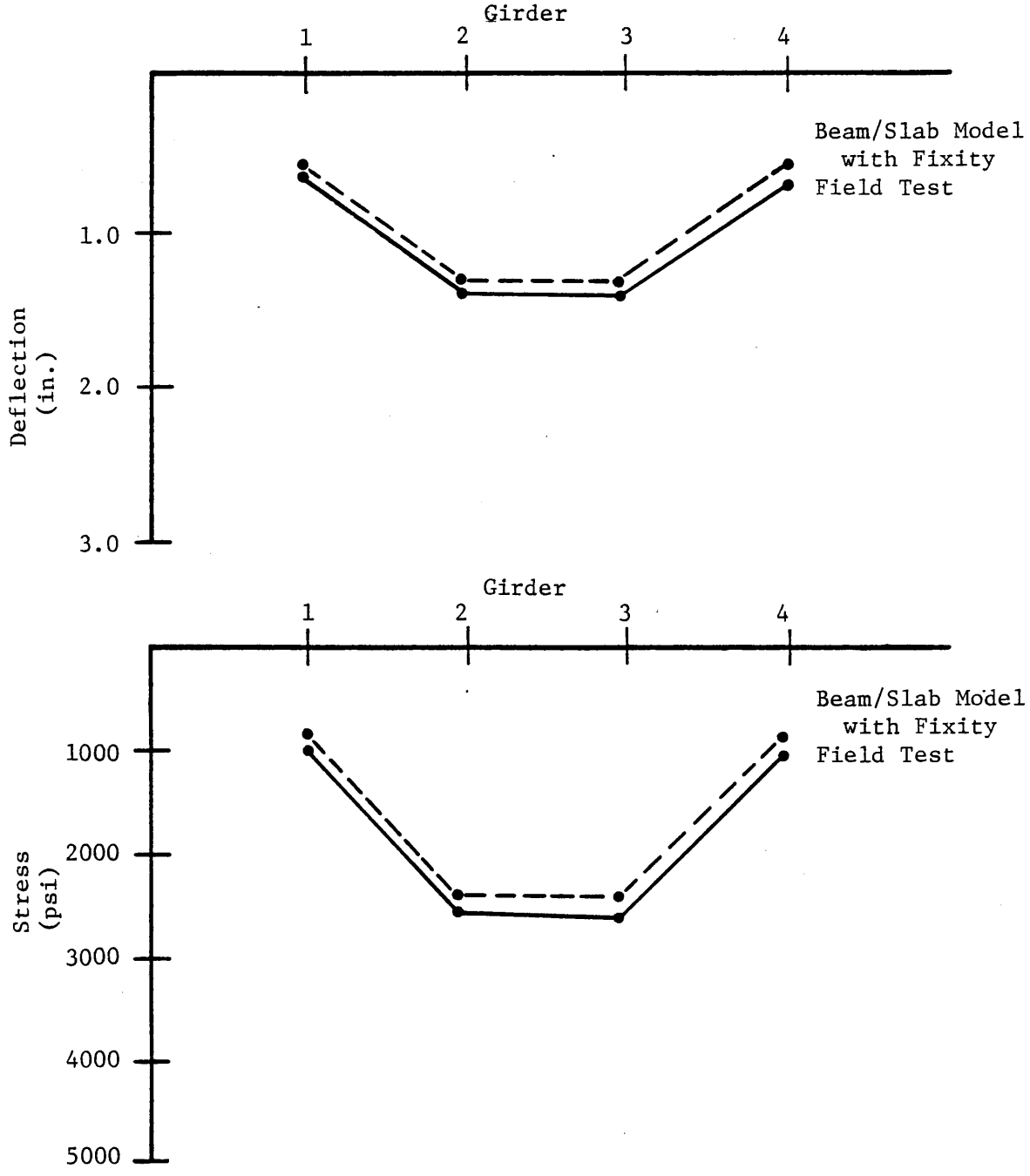

Figure 37. Plot of displacement and maximum stress at midspan -- Load Case 3-4.

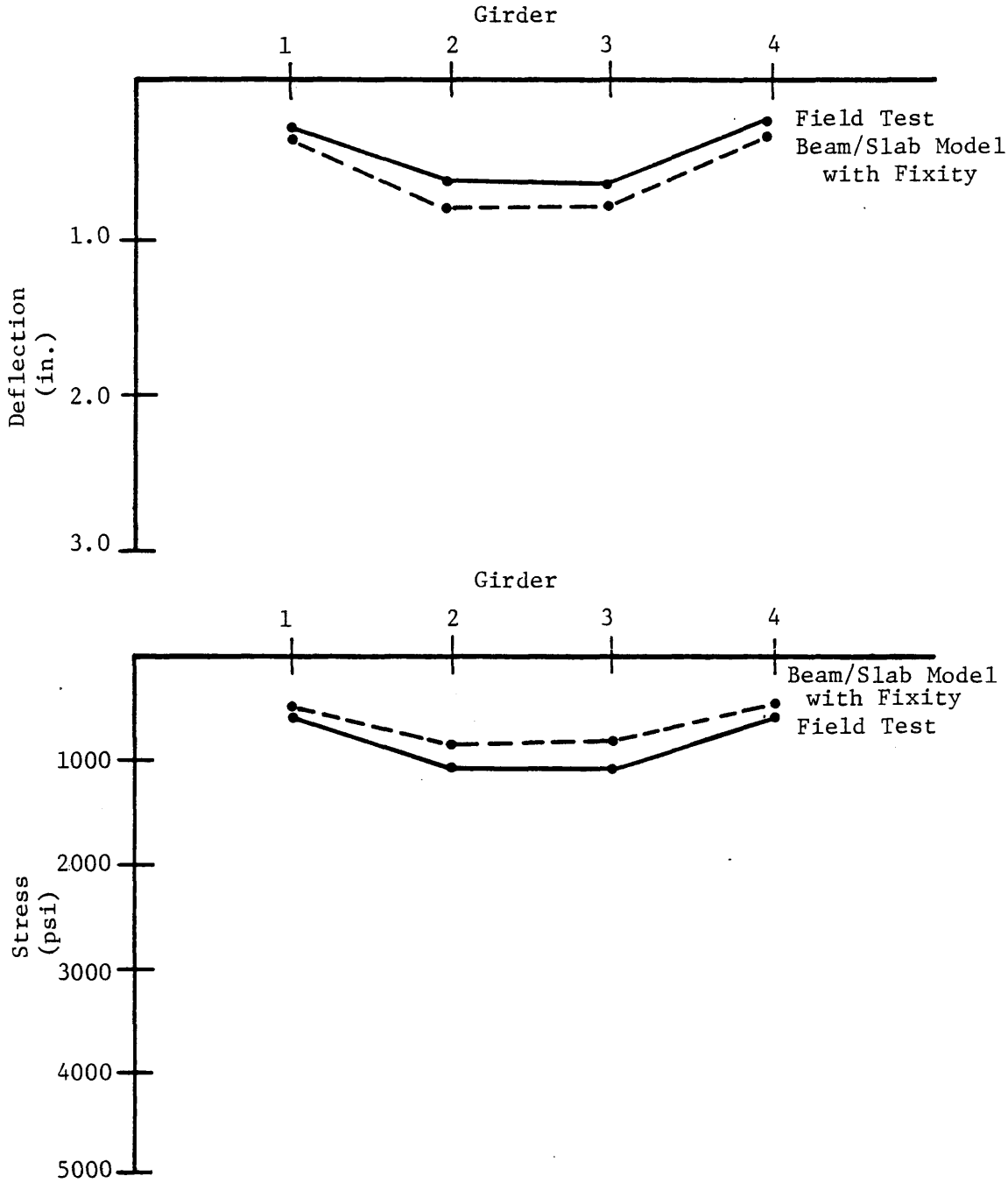

Figure 38. Plot of displacement and maximum stress at quarter point -- Load Case 3-4.

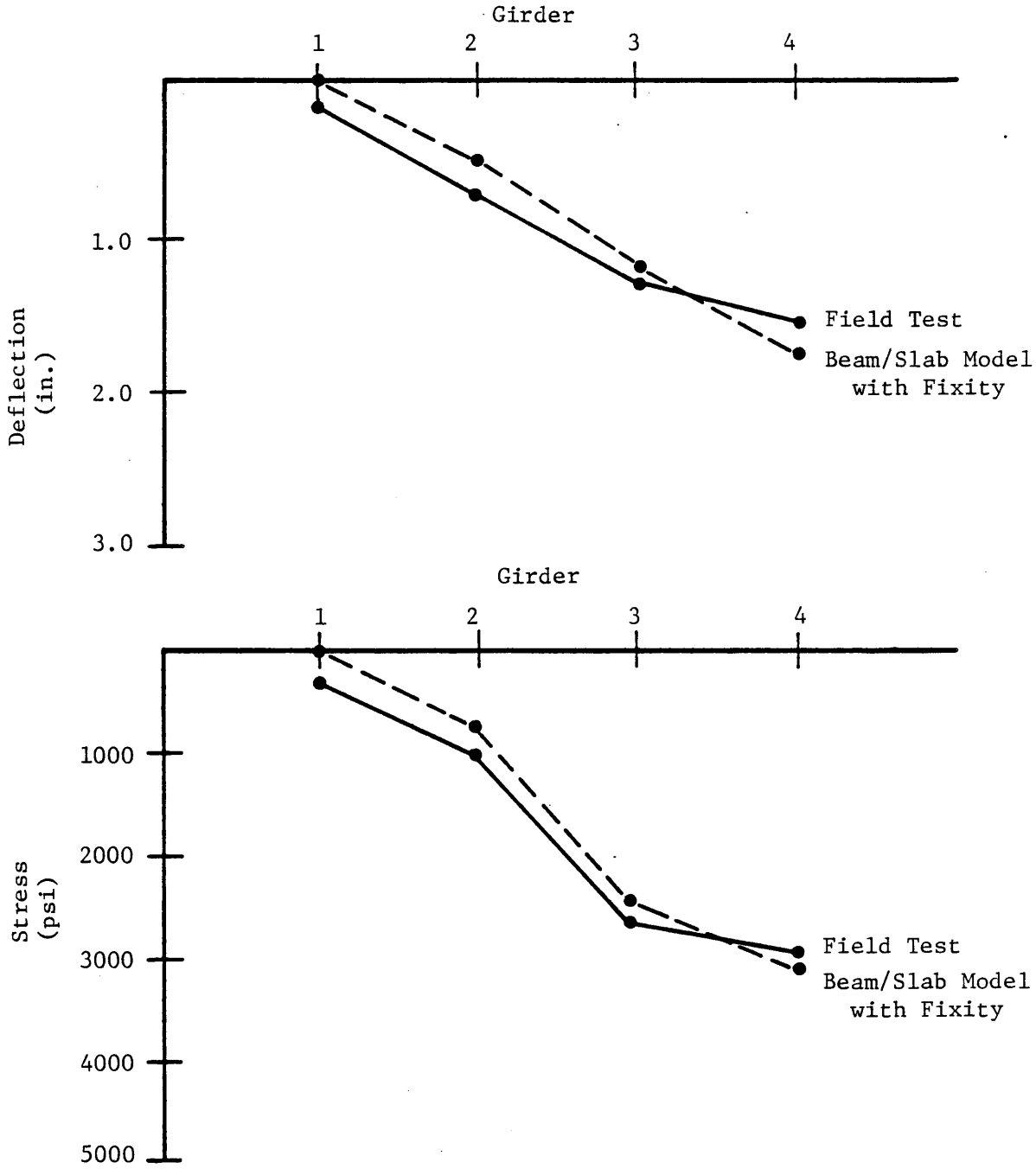

Figure 39. Plot of displacement and maximum stress at midspan -- Load Case 1-4.

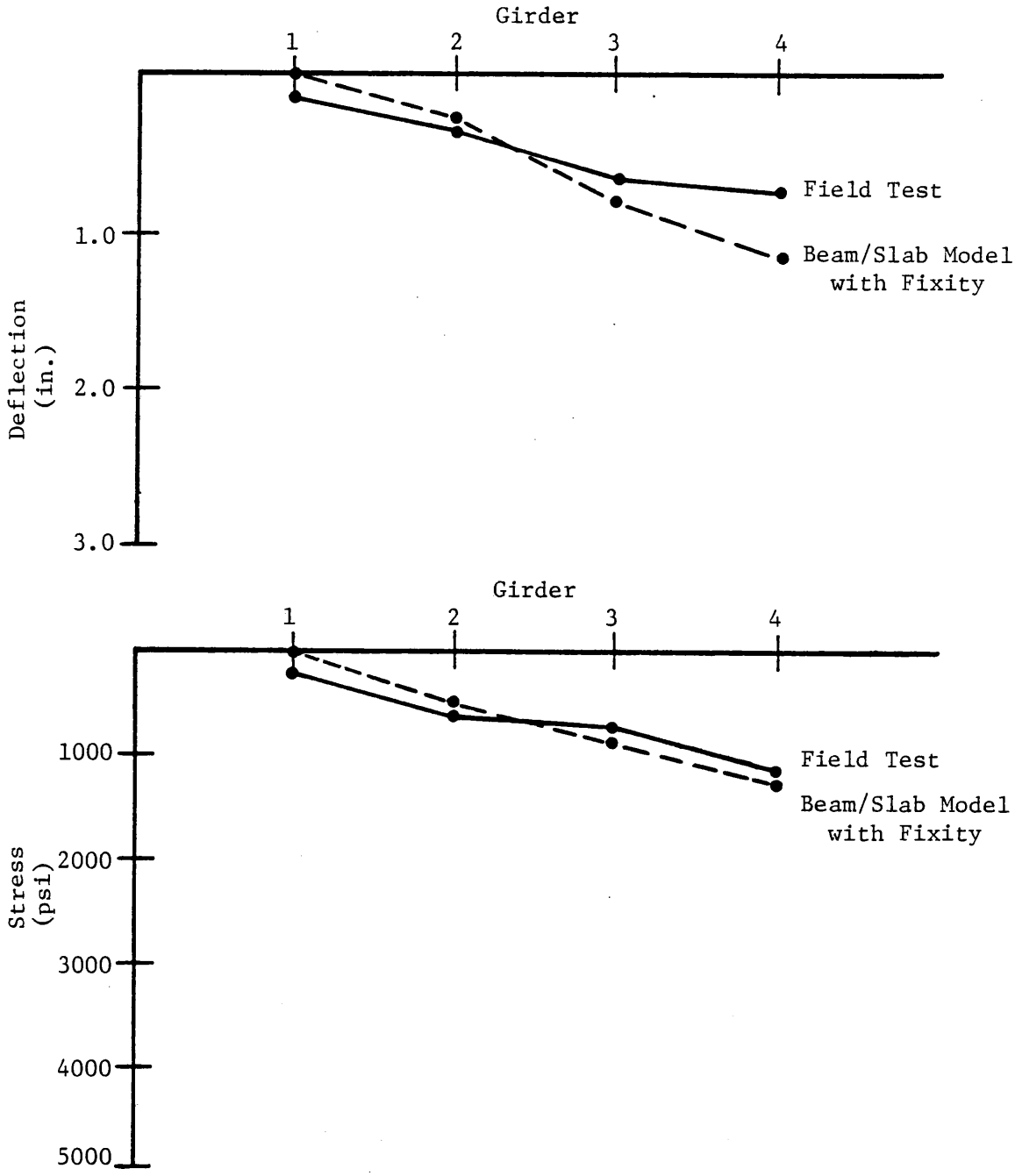

Figure 40. Plot of displacement and maximum stress at quarter point -- Load Case 1-4.

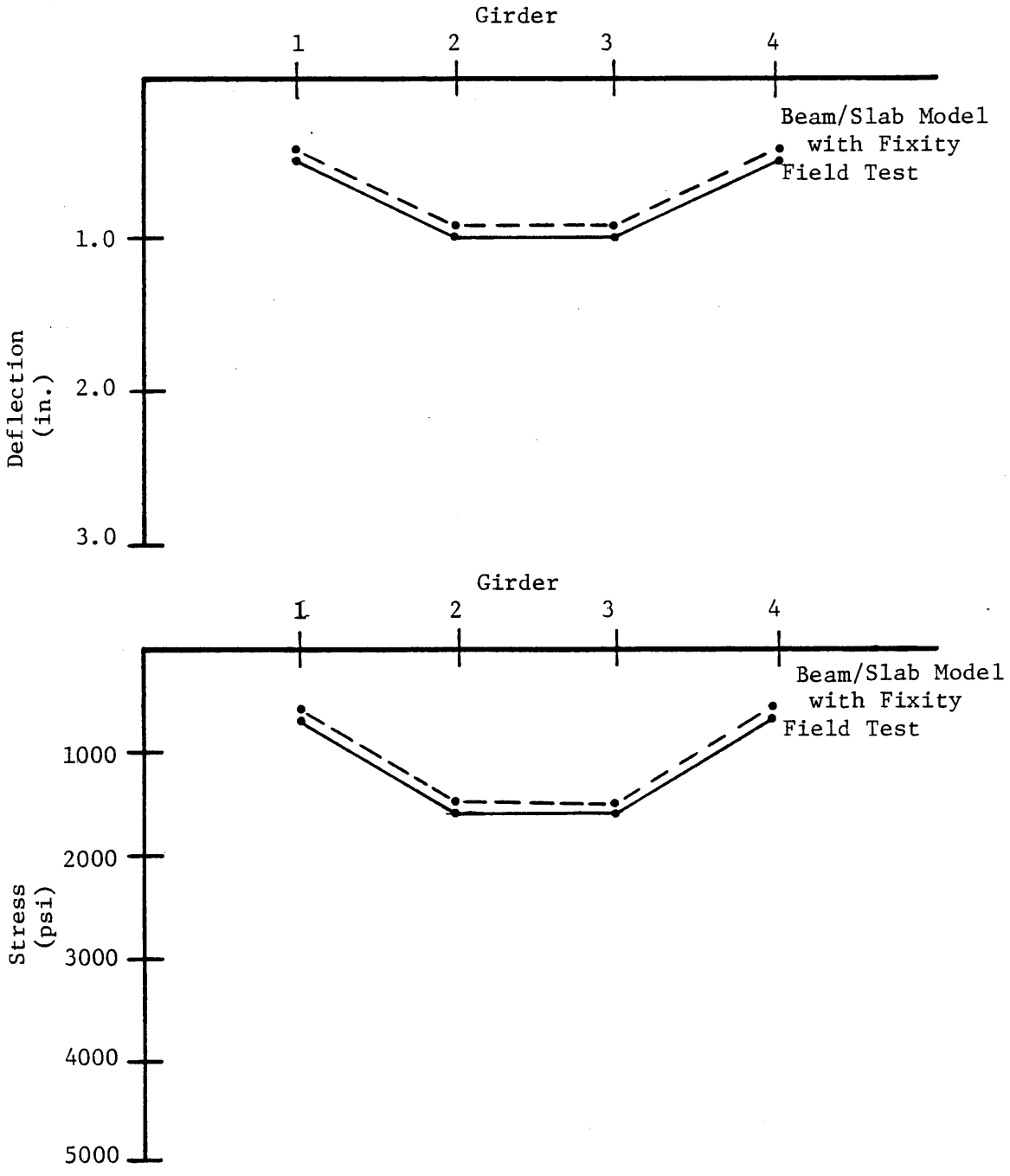

Figure 41. Plot of displacement and maximum stress at midspan -- Load Case 3-2.

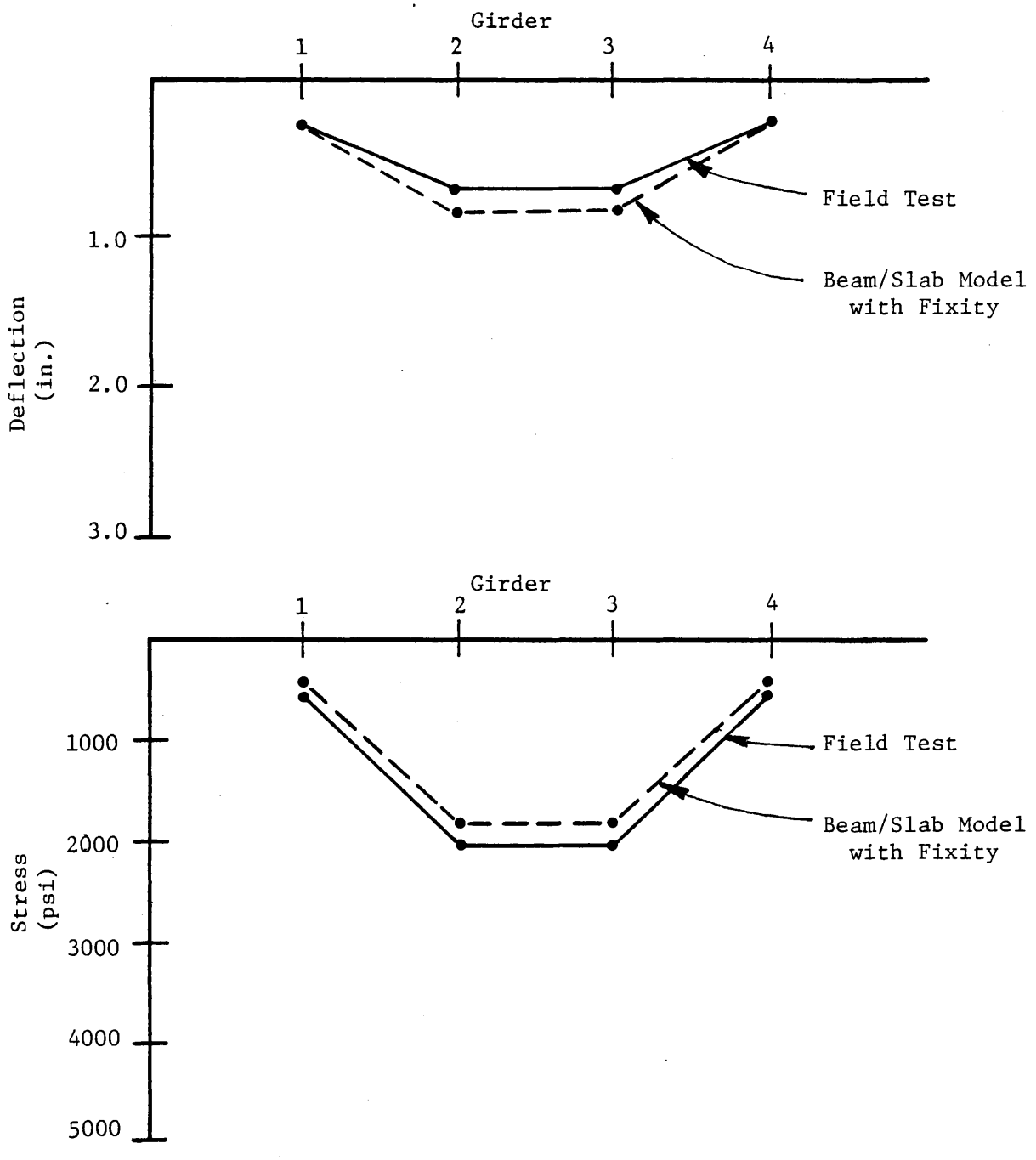

Figure 42. Plot of displacement and maximum stress at quarter point -- Load Case 3-2.

TABLE 11

Response of Plate/Slab Model

Load Case	Girder 1	2	3	4
		Displacements (in) at Quarter Point		
1-2	0.133	0.107	0.051	0.053
3-4	0.086	0.118	0.118	0.086
		Displacements (in) at Midspan		
1-2	0.160	0.133	0.086	0.056
3-4	0.115	0.177	0.177	0.115
		Stresses (psi) at Quarter Span		
1-2	2,090	1,830	1,210	910
3-4	1,270	1,420	1,420	1,270
		Stresses (psi) at Midspan		
1-2	2,390	1,680	910	520
3-4	1,340	2,540	2,540	1,340

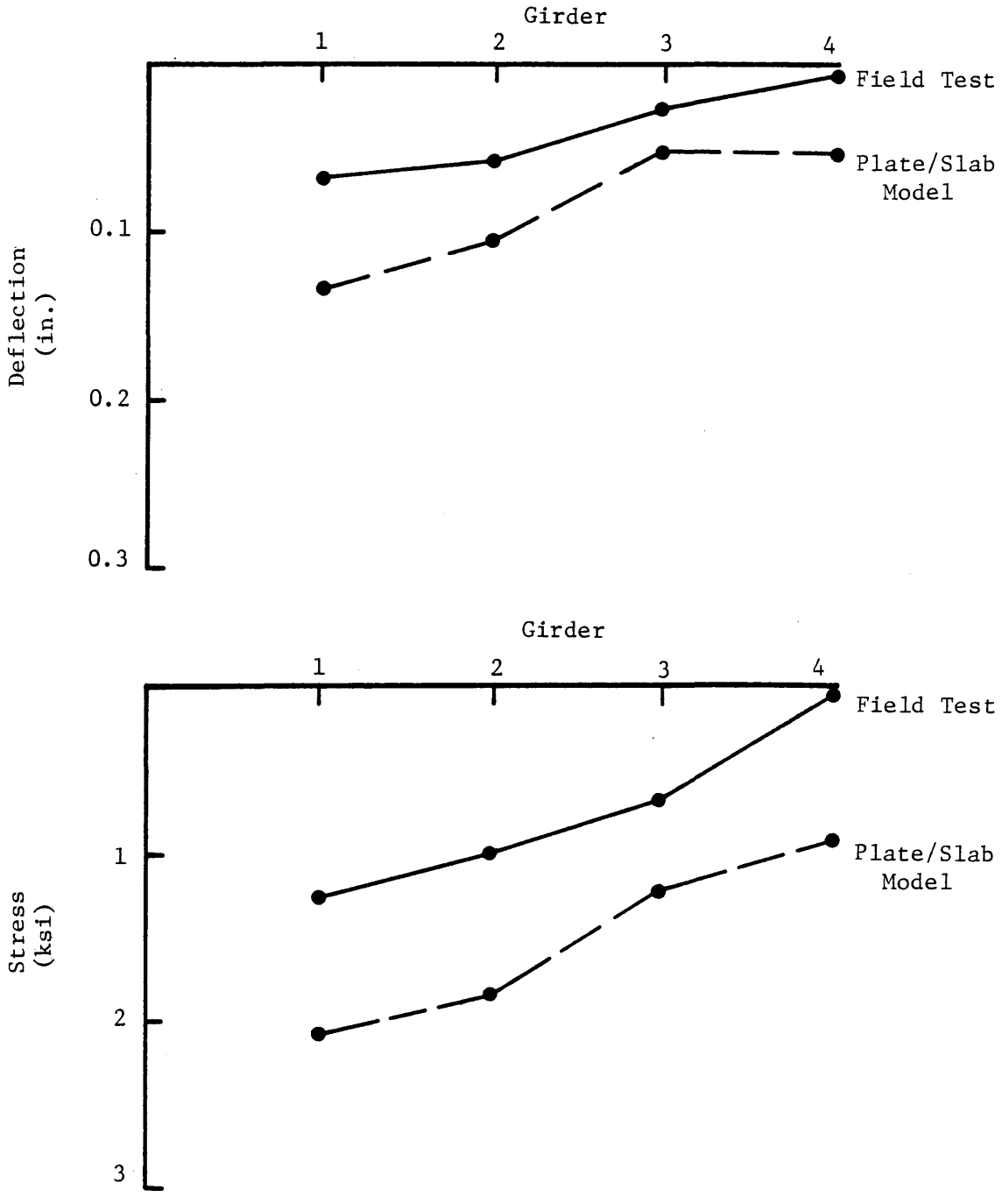

Figure 43. Plot of displacement and maximum stress at quarter point -- Load Case 1-2.

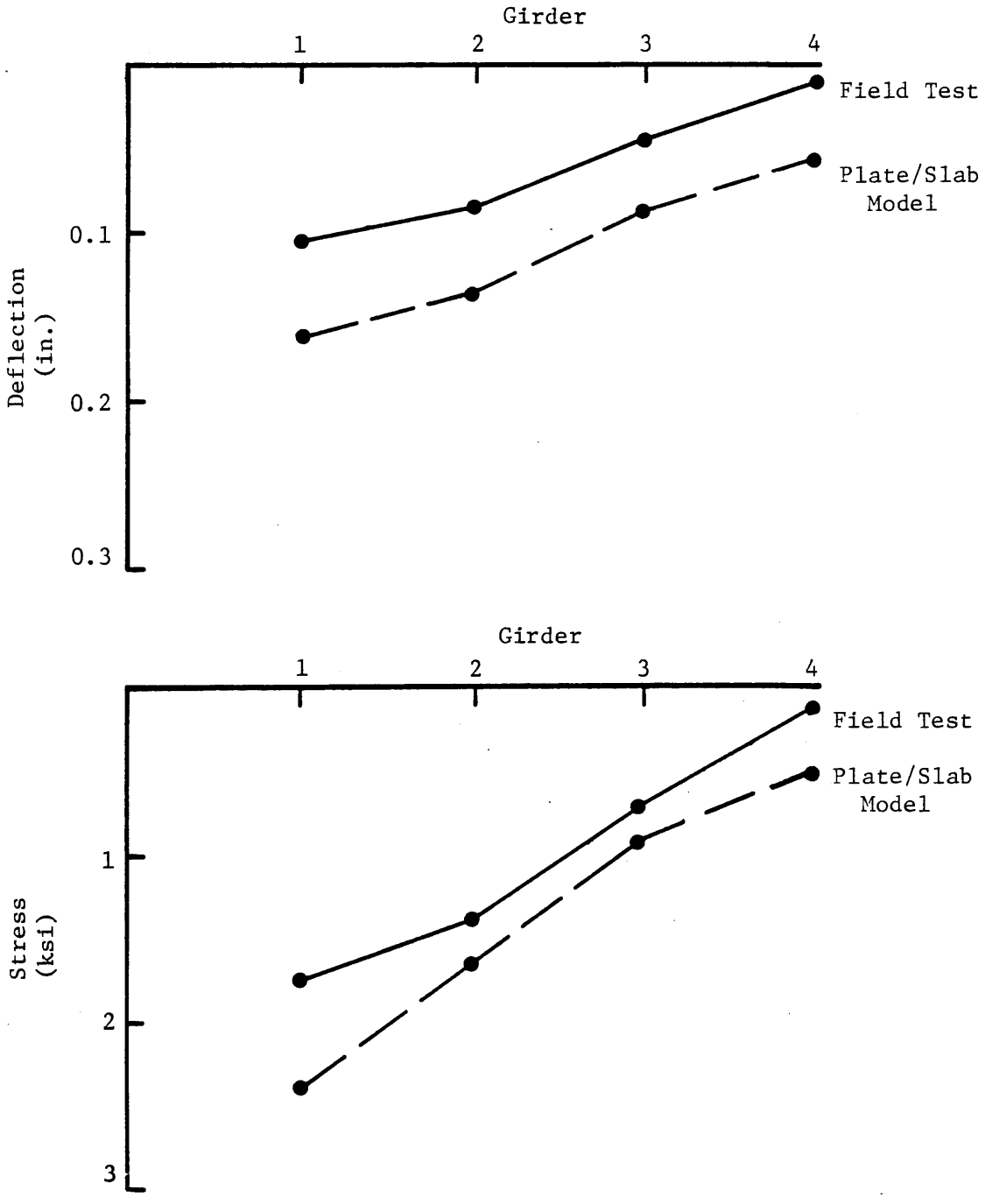

Figure 44. Plot of displacement and maximum stress at midspan -- Load Case 1-2.

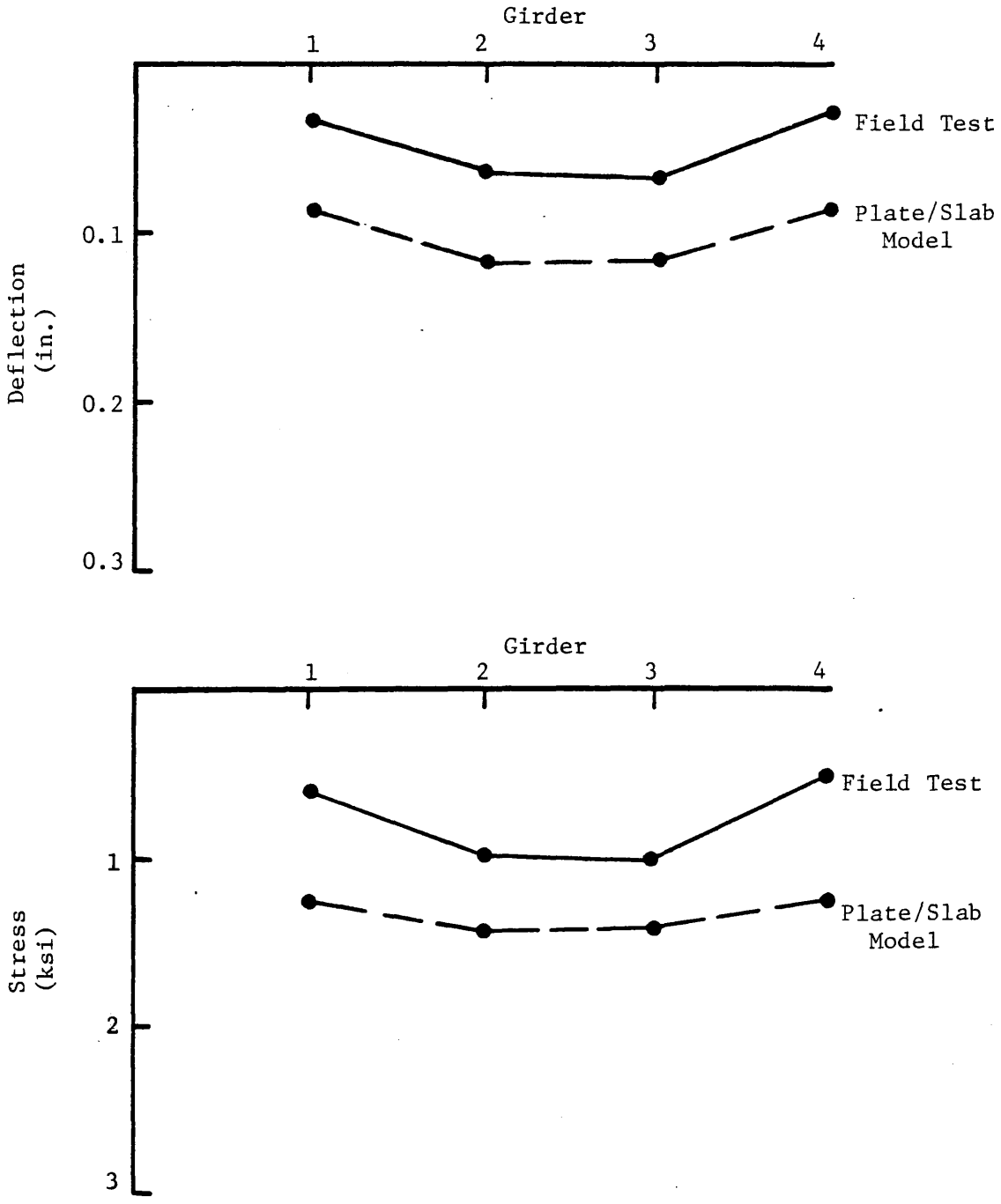

Figure 45. Plot of displacement and maximum stress at quarter point -- Load Case 3-4.

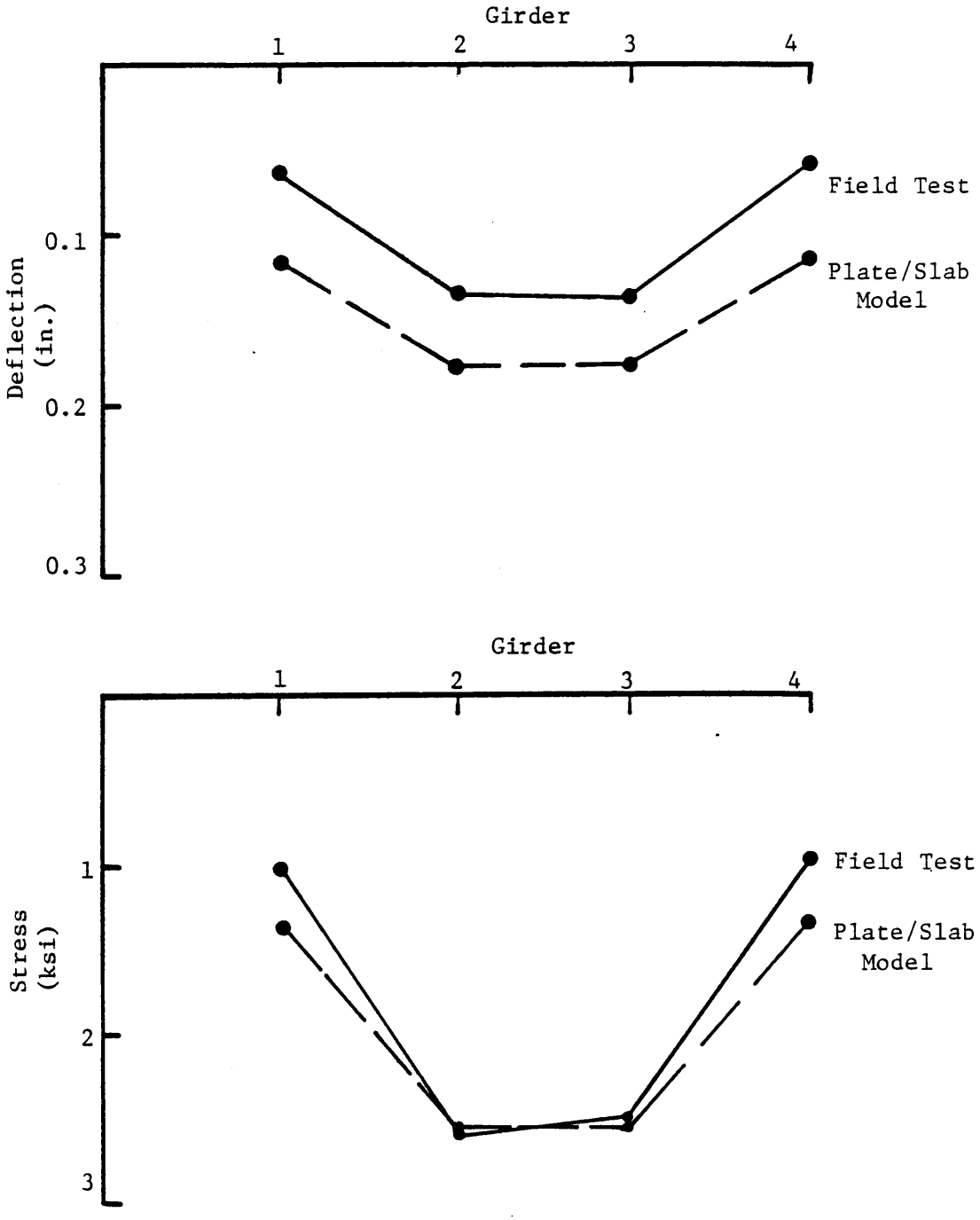

Figure 46. Plot of displacement and maximum stress at midspan -- Load Case 3-4.

This was particularly true for loads in the centerline lane, where the response was essentially symmetric. As was noted earlier, the predicted values of displacement were considered a more reliable basis for comparison than were the values of predicted stress. Both, however, are presented for completeness.

As may be observed from Figures 45 and 46, the general transverse distribution of deflections for load case 3-4 as predicted by the plate/slab model were very similar in shape to those measured in the field test, but significantly larger. For example, at midspan the maximum measured deflection was approximately 0.13 in while the maximum predicted value was approximately 0.18 in, a difference of some 40%. At the exterior girders, the difference was even more pronounced, with the predicted values exceeding the experimental by over 80 percent. The predicted displacement data at the quarter point for load case 3-4 was similar to the midspan data except that the differences between the measured and predicted values were somewhat larger. At the interior girders, the predicted displacements were approximately 80% larger than the experimental, while at the exterior girders, the predicted were almost three times the measured values. For load case 1-2, the predicted displacements at the quarter point and midspan again closely resembled the shape of the corresponding experimental values, as noted in Figures 43 and 44, although the differences were not quite as large.

The relationship between the predicted and measured stresses was similar to that observed for displacements, although the differences were not quite as large. It is likely that inconsistencies between the measured and predicted values of displacements and stresses were due to the particular modelling of the girders. It also appears that for both stresses and displacements, the largest discrepancy between the measured and predicted values occurred at the girders farthest from the load, which would indicate some deficiency in the transverse load distribution within the finite element models. However, the major shortcoming in the basic plate/slab model was the excessive longitudinal flexibility. Modifying the fixity at the supports and including the additional stiffness of the curb/railing were examined, since both of these factors could increase the overall longitudinal stiffness.

For this particular plate/slab model, support continuity or end fixity was implemented in the following manner. For a given load case, all nodes at both supports were fixed against rotation and the corresponding reaction moments calculated. In a subsequent analysis of the same load case, the rotational constraint was removed and an applied moment, equal to the reaction moment scaled by a fixity factor, was applied in addition to the vehicle loading. The fixity factor for each girder was selected to be the same as that measured in the field test.

The plate/slab model, modified to include partial fixity at the supports, was then reanalyzed for all of the load cases considered. For load case 3-4 and load case 1-2, stresses and displacements at the quarter point and midspan are tabulated in Table 12. For the symmetric loading (load case 3-4), adding partial fixity at the supports decreased the stresses and displacements on the order of 8% to 12%, while for load case 1-2, partial restraint at the support also resulted in reductions in stresses and displacements from zero to twenty percent. Based on these results, two conclusions become apparent. First, the addition of partial fixity at the supports in this model did not result in predicted stresses and displacements that compared favorably with the measured response data; thus additional modifications to the model apparently are necessary. Secondly, while the fixity factors were based on measured data, it is not clear how this experimental information should be translated into fixity factors at the ends of individual girders. Nevertheless, it is clear that some support restraint was present in the actual bridge and therefore should be included in some manner in the analytical model.

TABLE 12

Responses of Plate/Slab Model with Fixity

Load Case	Girder Locations 1	2	3	4
	Displacements (in) at Quarter Point			
1-2	0.120	0.096	0.062	0.044
3-4	0.078	0.108	0.107	0.074
	Stresses (psi) at Quarter Point			
1-2	1,850	1,660	1,050	820
3-4	1,220	1,290	1,280	1,030
	Displacements (in) at Midspan			
1-2	0.159	0.120	0.075	0.047
3-4	0.105	0.166	0.163	0.099
	Stresses (psi) at Midspan			
1-2	2,210	1,540	870	430
3-4	1,280	2,440	2,380	1,140

The remaining factor that could further reduce predicted displacements and thereby provide better correlation between the predicted response of the model and the measured response from the field test is the effect of the curb/railing component on the longitudinal stiffness of the model.

Initially, it was assumed that the curb/railing participated in the load-carrying capability of the bridge but only as a noncomposite unit with the deck. Including the railing in this manner produced essentially negligible changes in the stress and displacement responses, (less than 5%) for all loading conditions. This same negligible effect for noncomposite railing behavior was also observed for the beam/slab model. To further examine the effect of the railing, the stiffness of the railing was next included in the model, assuming fully composite behavior, together with the partial fixity effect. The responses of the plate/slab model, modified to include both of these factors, to load cases 3-4 and 1-2 are presented in Table 13. A plot of the displacements predicted by this model and measured experimentally for load cases 3-4 is shown in Figure 47. These results indicate the significant effect that including the composite railing had on the response of the plate/slab model. In fact, an examination of Figure 47, indicates that the best agreement between the displacement responses was achieved when both the composite railing and support continuity were included in the plate/slab model. This improvement was also true for stresses at the quarter point. However, the agreement between the predicted and measured stresses at midspan for both loading conditions was not favorable. For example, under load case 3-4, the predicted stresses were approximately 25% less than the measured values. However, for the basic plate/slab model with no support continuity and no railing effect, the stresses at midspan as predicted by the model agreed closely with the experimental values.

It is likely that displacements predicted by a finite element model of a bridge are more reliable than corresponding stresses. However, since the design, evaluation, and rating are dependent on stresses, it is essential that any analytical model adopted be capable of reasonable stress predictions.

TABLE 13

Response of Plate/Slab Model with Curb/Railing and Fixity

Load Case	Girder Locations 1	2	3	4
	Displacements (in) at Quarter Point			
1-2	0.078	0.070	0.045	0.021
3-4	0.051	0.086	0.086	0.048
	Stresses (psi) at Quarter Point			
1-2	1,330	1,320	760	460
3-4	820	1,020	1,010	620
	Displacements (in) at Midspan			
1-2	0.107	0.090	0.054	0.027
3-4	0.071	0.137	0.134	0.065
	Stresses (psi) at Midspan			
1-2	1,490	1,270	730	290
3-4	940	2,080	2,010	900

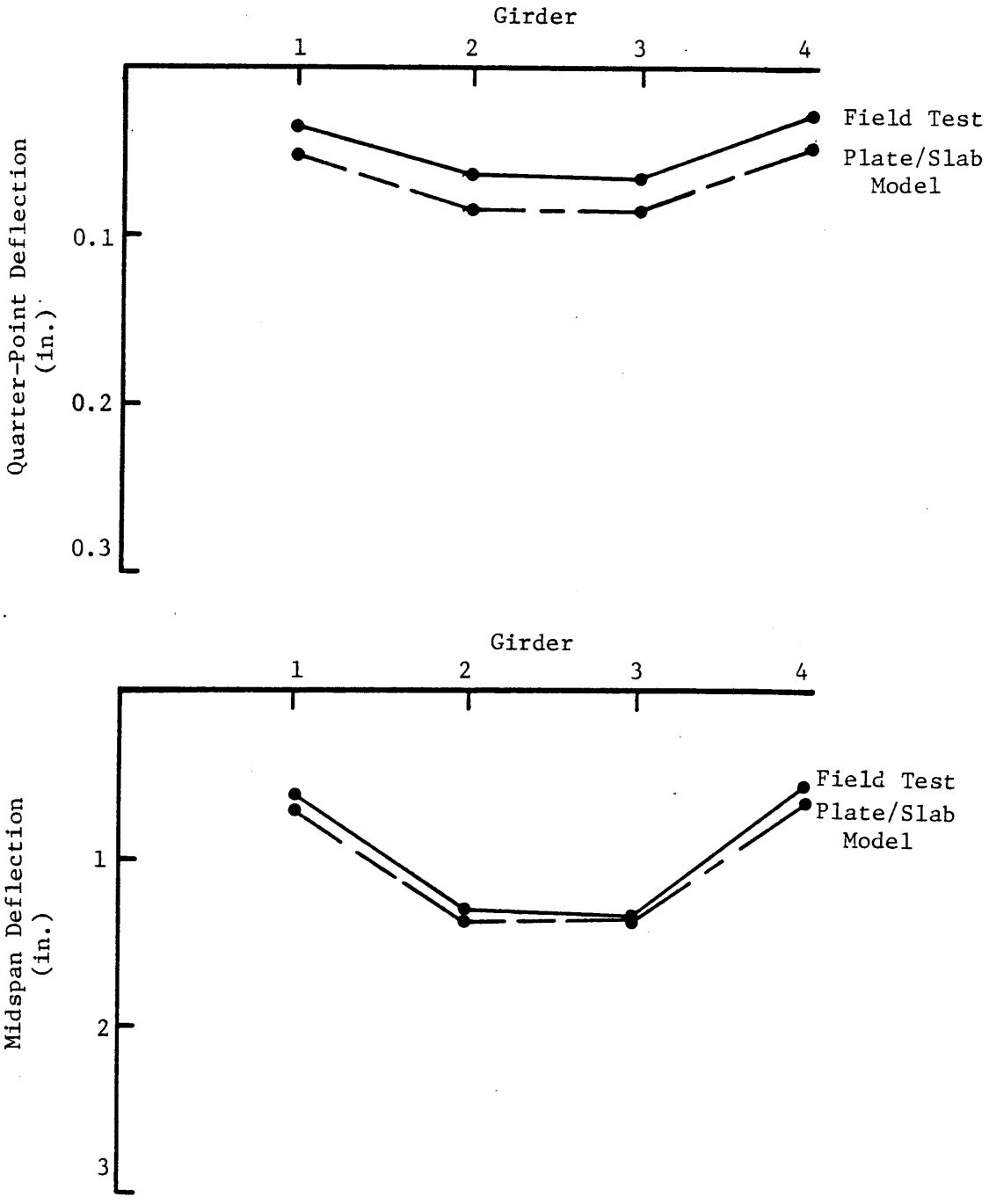

Figure 47. Plot of deflections from Plate/Slab Model including Curb/Railing and Fixity -- Load Case 3-4.

CONCLUSIONS

The purpose of this study was to develop an improved capability for predicting the stress and displacement response of a highway bridge to prescribed vehicle loads. This was accomplished by using experimental bridge response, measured during a controlled field test, as a guide for the development and formulation of a simple but realistic finite element model of the bridge. The final computer model developed with the aid of this experimental data, was able to predict displacements and stresses that compared favorably with the measured data for this particular bridge. This final section of the report briefly summarizes the pertinent findings of this study and identifies conclusions drawn from both the experimental and analytical phases of the investigation.

The experimental response measured during the field test was essentially what would have been expected with one exception, and this feature was not immediately obvious. In reviewing the data, it was observed that vehicle loadings in one span resulted in measurable stresses and displacements in an adjacent span. This behavior occurred even though all spans in the structure were designed and constructed as simply-supported spans. Further evidence of this continuity at the supports was found in the analysis of the live load stresses (see Table 4). As part of this analysis, the resisting moment in the span, for a particular loading, was calculated based on measured stresses and properties of the slab and girders. For this same loading, a theoretical applied moment was determined, based on statics and assuming simply-supported ends. It was found that the resisting moment was substantially less than the theoretical applied moment, suggesting that there must have been some fixity at the supports which would have markedly reduced the calculated applied moment. The existence of support fixity was further substantiated by subsequent visual examination of the bearings where severe corrosion, sufficient to restrain rotation was observed. Such a support condition, while not detrimental in itself, would have a significant effect on analyses used for predicting response or capacities.

The initial finite element models developed to represent the bridge span predicted response values which did not compare favorably with measured response. However, these models, derived to best represent the physical and geometric characteristics of the bridge, included boundary conditions intended to represent hinged and pinned boundaries. Detailed evaluation of the predicted response of the finite element models clearly indicated that slight variations of most model parameters, within reasonable ranges, had little effect on predicted response. However, when the boundary conditions of the model were changed to represent as closely as possible the actual support conditions as indicated by field test measurements, it was found that the predicted response was in surprising agreement with that determined in the field test, with deflections showing the closest agreement.

The results of this study have shown that the response of an actual bridge structure, and thus its capacity, can be satisfactorily predicted using rationally developed finite element models of the structure. Thus, the bridge engineer has the capability of determining response under particular loads, or of predicting capacities for certain structures. However, this study also points out the absolute necessity of understanding the actual characteristics and support mechanisms of the structure before a reliable model can be developed.

ACKNOWLEDGEMENTS

The authors gratefully acknowledge the contributions of Henry L. Kinnier, faculty research engineer, who was deeply involved in the project, particularly in supervising the field test, prior to his retirement in June 1985. Much of the model development that forms the basis of the theoretical approach to determining the capacity of a bridge was performed by Roy M. Sullivan and Mark H. Williford, graduate research assistants supported by the project. James W. French, materials technician supervisor, played a major role in the accomplishment of the field work; and John Reisky de Dubnic assisted in the field test and the initial data reduction. Finally, the authors thank Arlene Fewell for her patience and competence in typing the many drafts of this report.

The extensive field work required the cooperation of several persons from the Federal Highway Administration and the Staunton District of the Virginia Department of Highways & Transportation, without whom the project could not have been completed. Harry Laatz and Ron Nelson of the FHWA supervised the installation of the strain and deflection gages, and provided and operated the recording equipment; and R. L. Moore, L. L. Misenheimer, and J. F. Dunkum of the Staunton District provided vital support throughout the field tests.

REFERENCES

1. Kinnier, H. L., "A Dynamic Stress Study of the Weyers Cave Bridge, Progress Report No. 2, Vibration Survey of Composite Bridges, Virginia Highway & Transportation Research Council, Charlottesville, Virginia, August 1963.

2. Bathe, K., E. L. Wilson, and F. E. Peterson, "SAP IV, A Structural Analysis Program for Static and Dynamic Response of Linear System," Report No. EERC 73-12, Earthquake Engineering Research Center, Berkeley, California, April 1974.

3. Whetstone, W. D., "SPAR Structural Analysis System Reference Manual," NASA CR-158970-1, National Aeronautics and Space Administration, November 1978.

4. Deslavo, D. J., and J. A. Swanson, "ANSYS Engineering Analysis System Users Manual," SASI, June 1985.